Imaging techniques for low-dose X-ray CT based on hybrid pixels : Compressed-sensing, a solution ?

Yannick Boursier - Groupe imXgam

Centre de Physique des Particules de Marseille

Journée du Traitement du Signal et de l'Image pour le Biomédical
10 septembre 2010

I - Biomedical at CPPM

CPPM : a lab from IN2P3 for particle physics.

Physics experiences : Antares, Atlas, LHCb, D0, ... and imXgam !

Some imXgam projects :

XPIX :

Hybrid pixels for X-ray : XPAD cameras.

PIXSCAN :

Micro CT-Scanner based on hybrid pixels.

ClearPET/XPAD :

Simultaneous PET/CT imaging based on hybrid pixels.

Outline

- 1- Biomedical imaging based on hybrid pixels
- 2 - Tomography reconstruction
- 3 - Future challenges. Sparsity and Compressed Sensing ?
- 4 - Conclusion

Hybrid pixel detectors for High Energy Physics

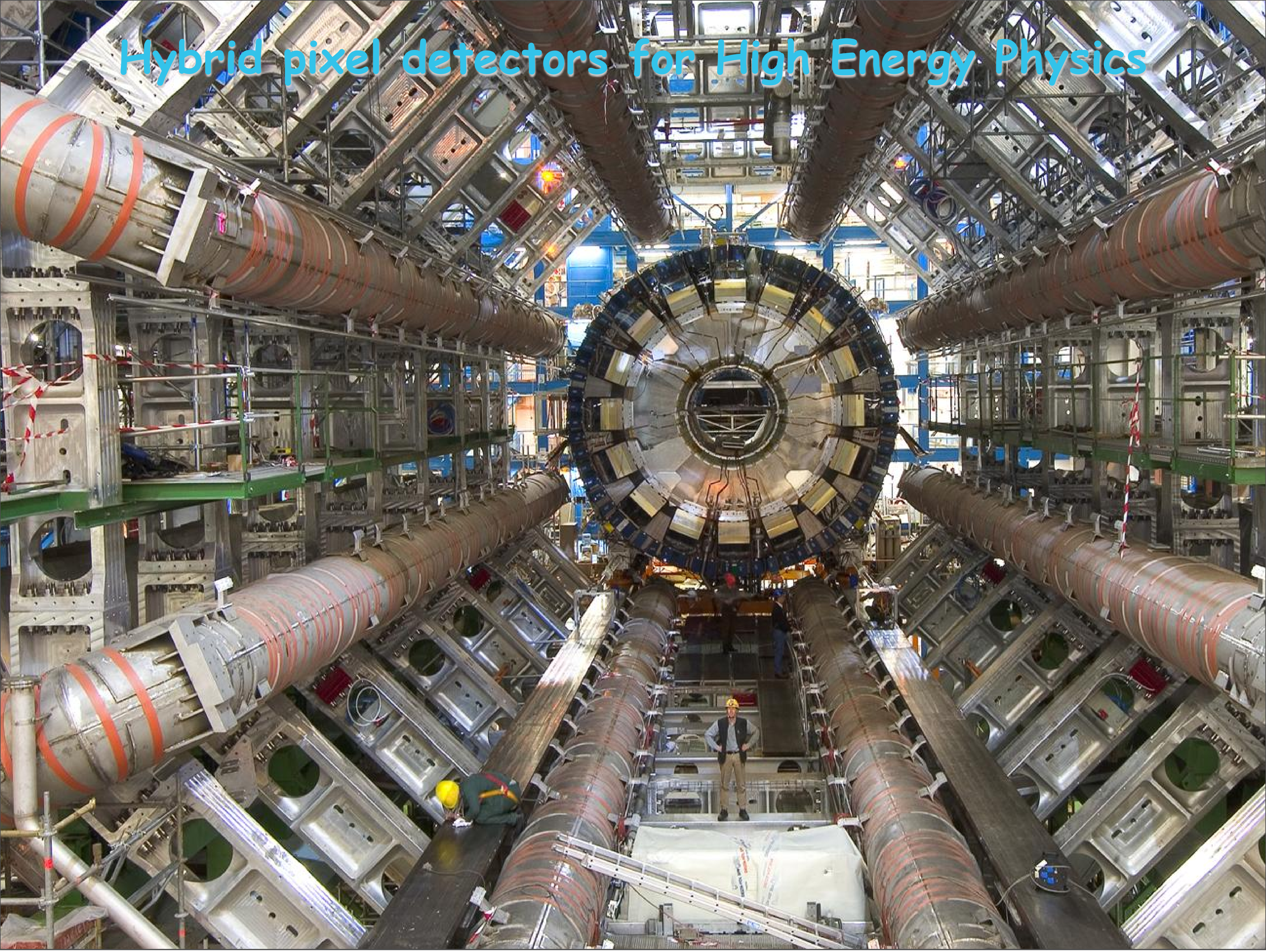

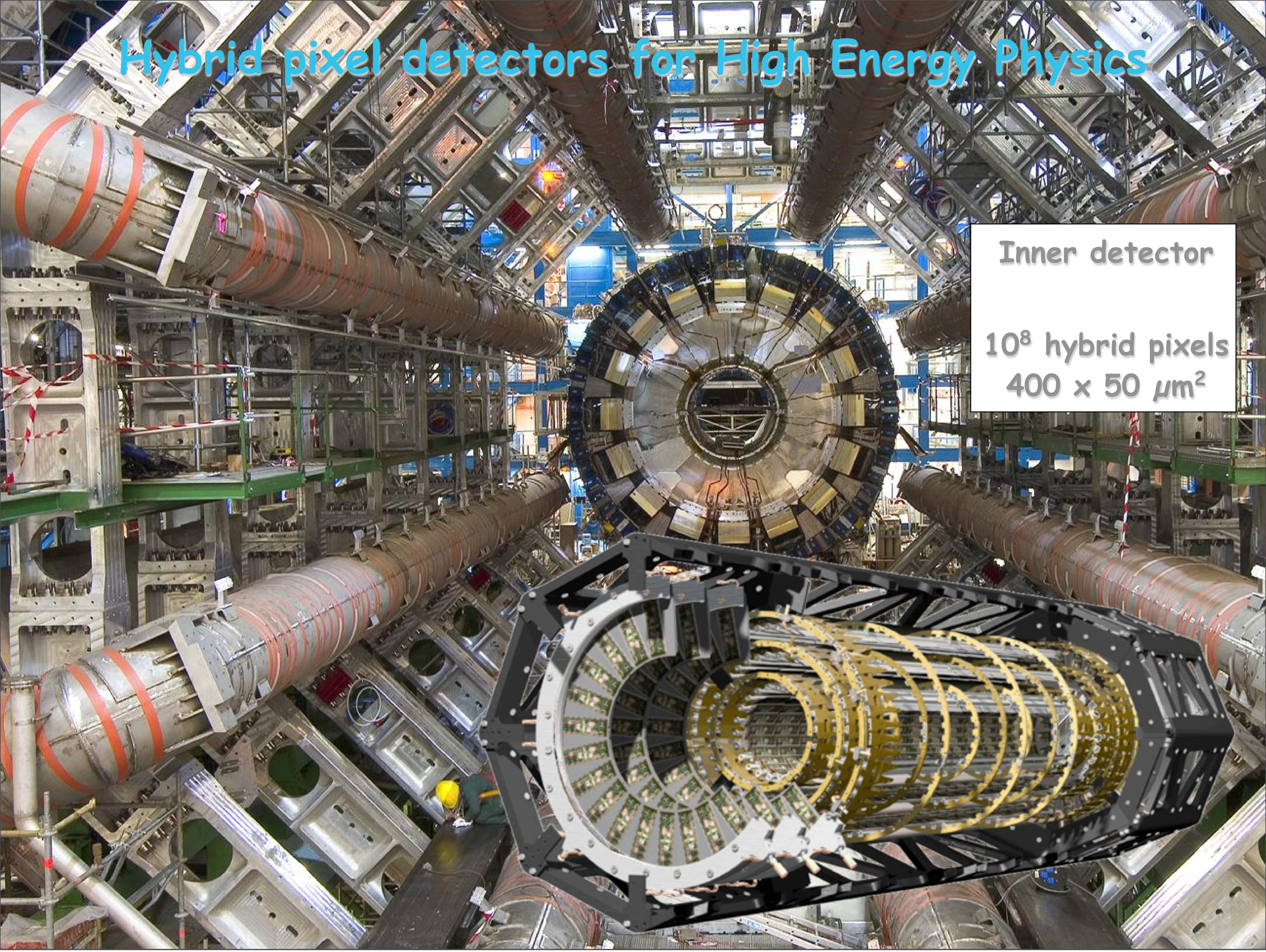
Hybrid pixel detectors for High Energy Physics
Inner detector
10^8 hybrid pixels
$400 \times 50\ \mu m^2$

Hybrid pixels

Hybrid pixel

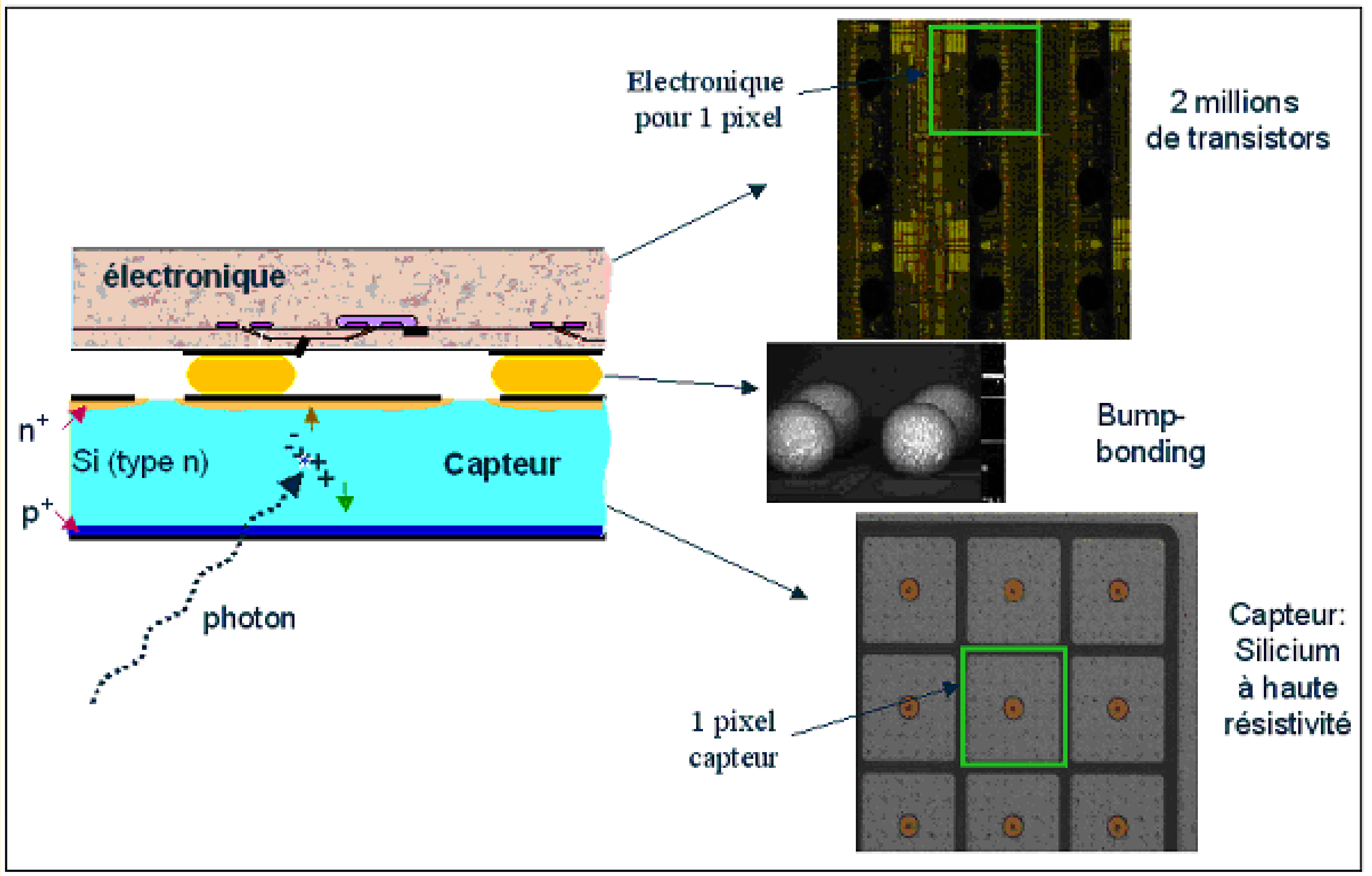

CCD

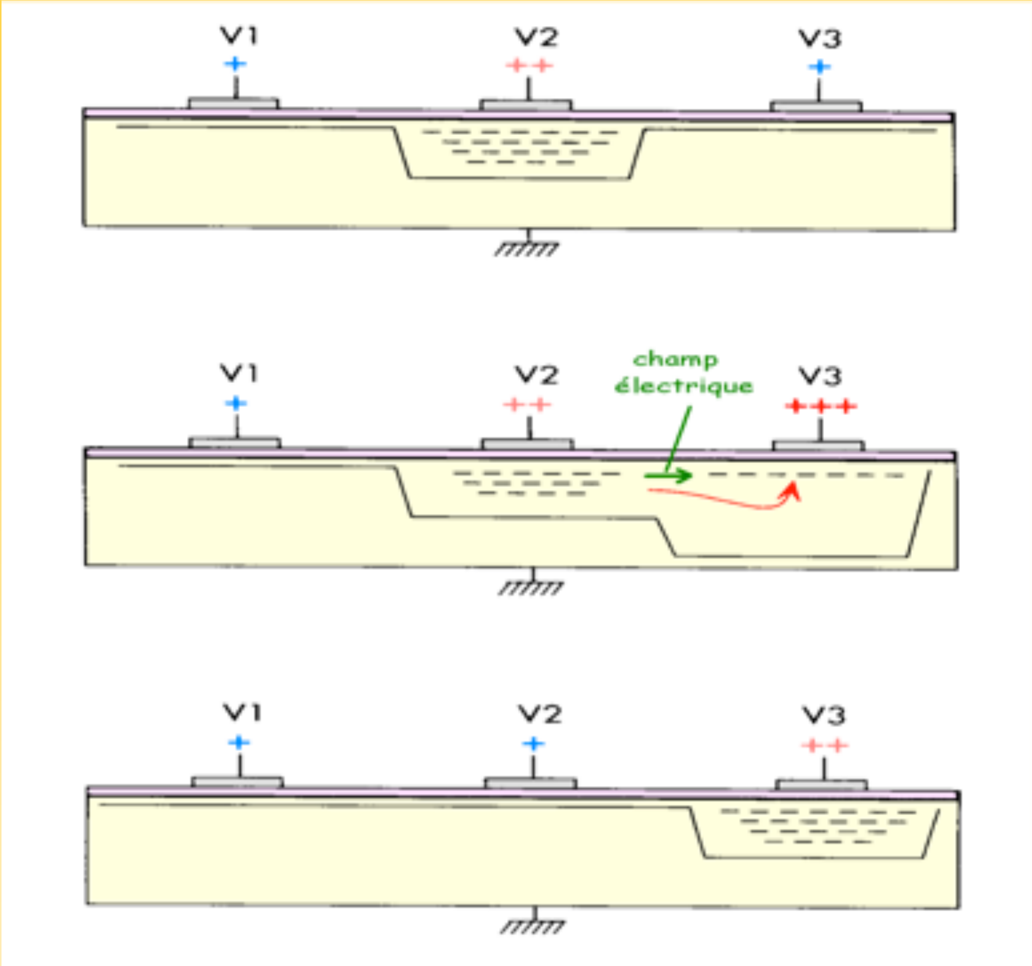

Fundamental difference with other detectors (CCDs-like) :

Photon counting mode !

No charge integration !

Hybrid pixels

Hybrid pixel

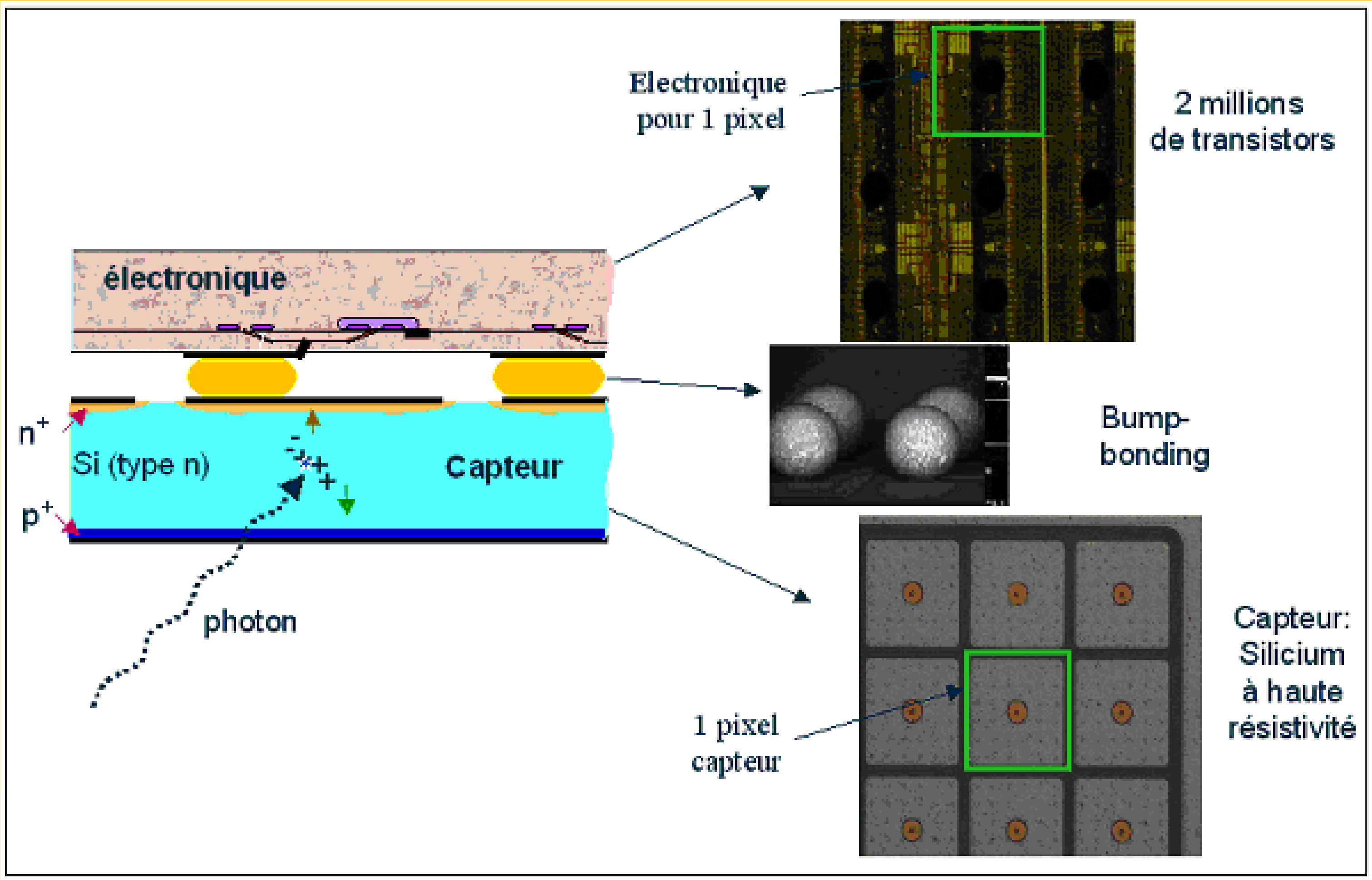

CCD

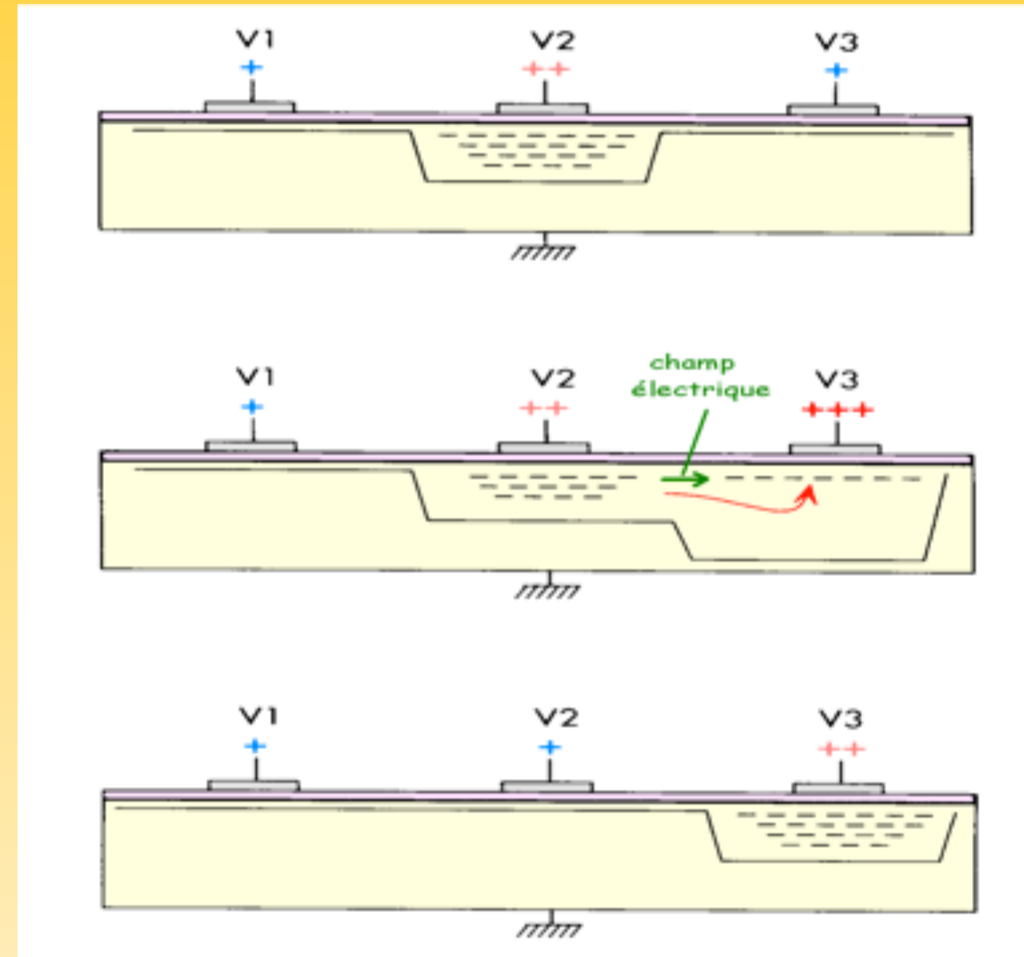

Fundamental difference with other detectors (CCDs-like) :

Photon counting mode !

No charge integration !

- No Dark noise
- Energy selection
- Very large dynamic range

Hybrid pixels

Hybrid pixel

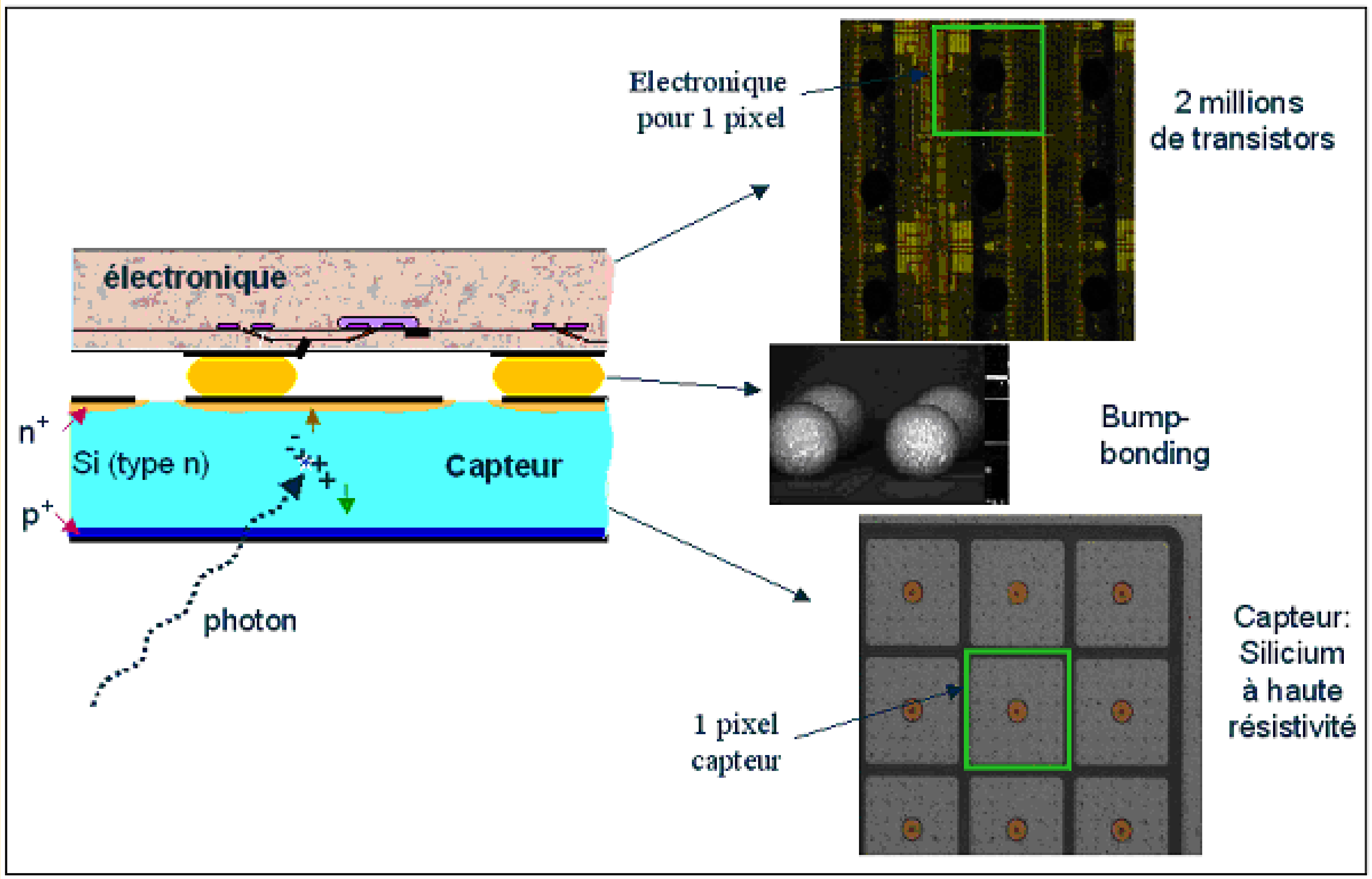

CCD

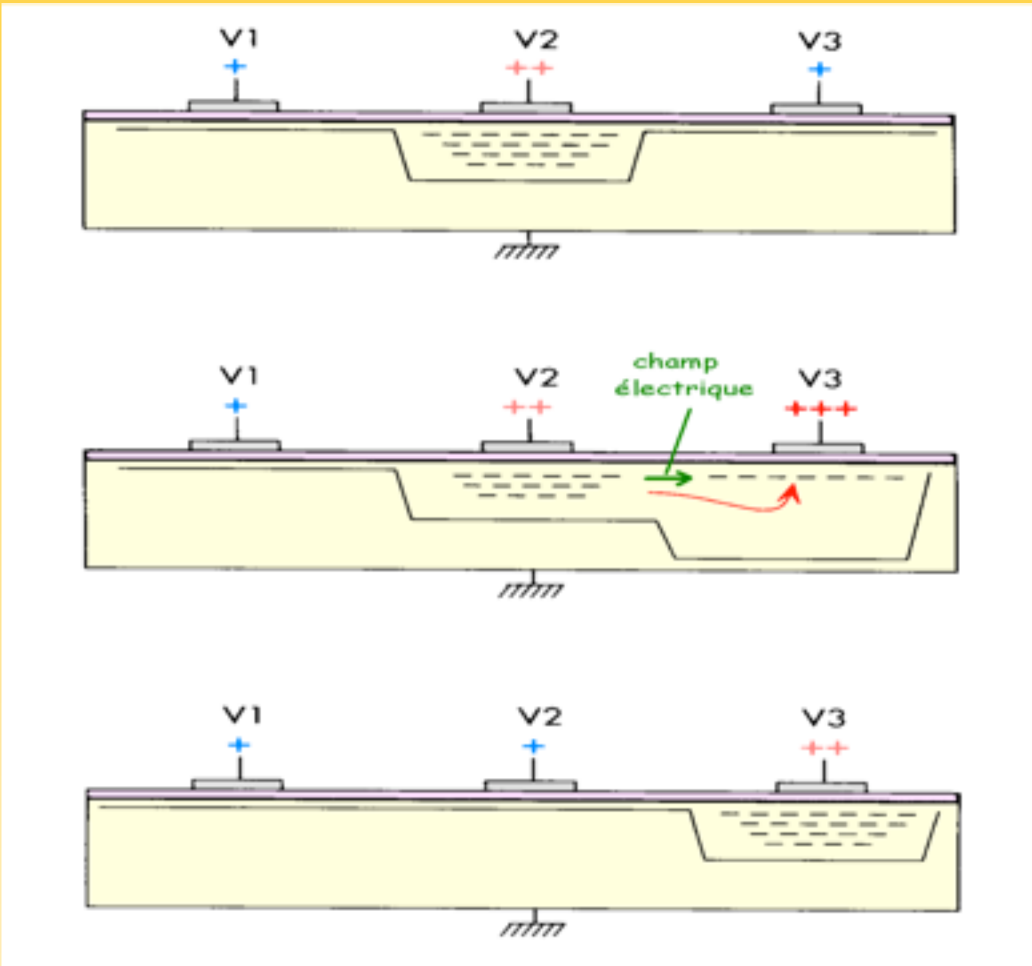

- very fast data acquisition
- choice of du substrat (Si, CdTE, AsGa)

  - No Dark noise
  - Energy selection
  - Very large dynamic range

Fundamental difference with other detectors (CCDs-like) :

Photon counting mode !

No charge integration !

Photon counting versus charge integration

Photon counting versus charge integration

Photon counting mode

Energy threshold of detection

Choice of sensor

Photon counting versus charge integration

Photon counting mode

- Very low couting rate

Energy threshold of detection

Choice of sensor

Photon counting versus charge integration

Photon counting mode

- ✓ Very low couting rate

(0,01 ph/pixel/s)

Energy threshold of detection

Choice of sensor

Photon counting versus charge integration

Photon counting mode

- ✓ Very low couting rate (0,01 ph/pixel/s) → **Low statistics**

Energy threshold of detection

Choice of sensor

Photon counting versus charge integration

Photon counting mode

- ✓ Very low couting rate
(0,01 ph/pixel/s) → **Low statistics**

- ✓ Large dynamic range
(10^{-2} - 10^{6} ph/pixel/s , 80dB)

Energy threshold of detection

Choice of sensor

Photon counting versus charge integration

Photon counting mode

- ✓ Very low couting rate (0,01 ph/pixel/s) → **Low statistics**
- ✓ Large dynamic range (10^{-2} - 10^{6} ph/pixel/s , 80dB) → **Enhanced detectability at low contrast**

Energy threshold of detection

Choice of sensor

Photon counting versus charge integration

Photon counting mode

- Very low couting rate (0,01 ph/pixel/s) → **Low statistics**
- Large dynamic range (10^{-2} - 10^{6} ph/pixel/s , 80dB) → **Enhanced detectability at low contrast**

Energy threshold of detection

- Energy selection of X-rays

Choice of sensor

Photon counting versus charge integration

Photon counting mode

- ✓ Very low couting rate (0,01 ph/pixel/s) → **Low statistics**
- ✓ Large dynamic range (10^{-2} - 10^{6} ph/pixel/s , 80dB) → **Enhanced detectability at low contrast**

Energy threshold of detection

- ✓ Energy selection of X-rays → Discriminating diffused photons → **Enhanced contrast**

Choice of sensor

Photon counting versus charge integration

Photon counting mode

- ✓ Very low couting rate (0,01 ph/pixel/s) → **Low statistics**
- ✓ Large dynamic range (10^{-2} - 10^{6} ph/pixel/s , 80dB) → **Enhanced detectability at low contrast**

Energy threshold of detection

- ✓ Energy selection of X-rays → Discriminating diffused photons → **Enhanced contrast**

Choice of sensor

- ✓ High density sensors

Photon counting versus charge integration

Photon counting mode

- Very low couting rate (0,01 ph/pixel/s) → **Low statistics**
- Large dynamic range (10^{-2} - 10^{6} ph/pixel/s , 80dB) → **Enhanced detectability at low contrast**

Energy threshold of detection

- Energy selection of X-rays → Discriminating diffused photons → **Enhanced contrast**

Choice of sensor

- High density sensors → Better detection efficiency → **Enhanced detectability + Low statistics**

XPAD3 camera : more than 500,000 pixels of 130 µm

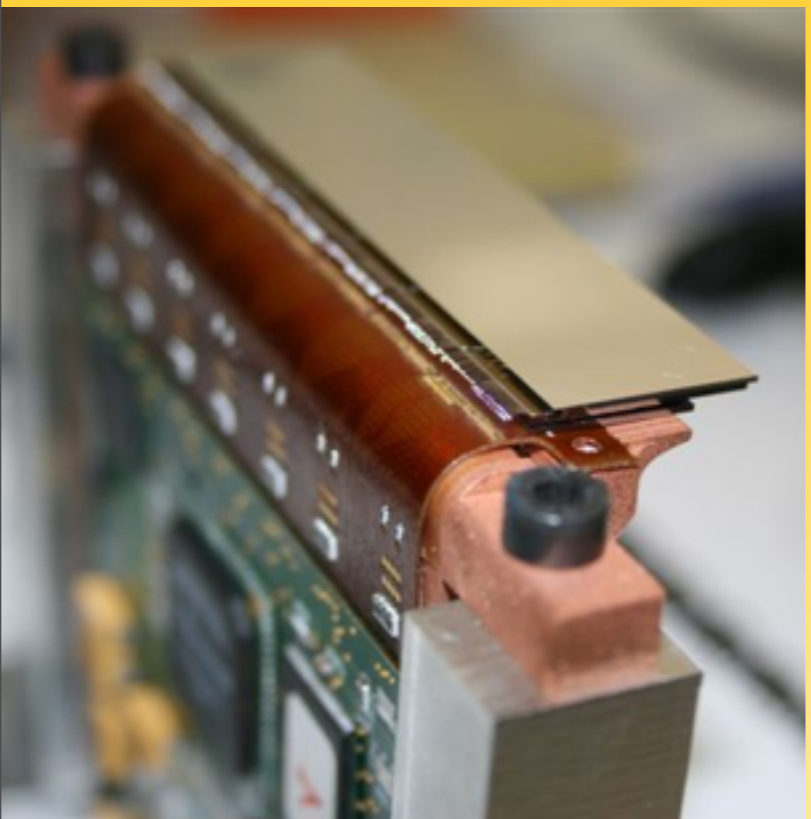

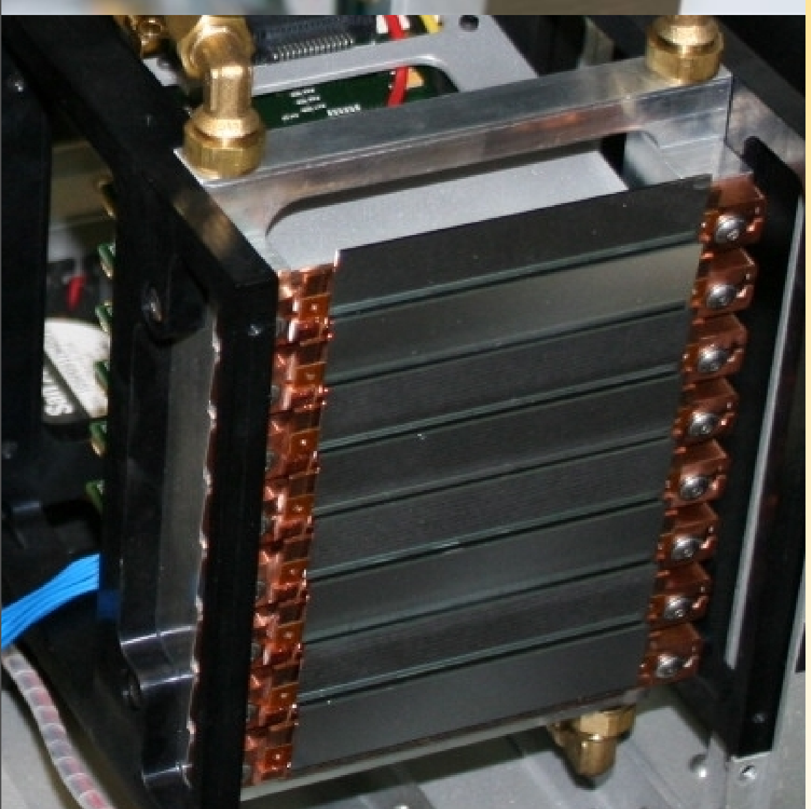

New hybrid pixel camera for X-rays XPAD3/Si

- Photon couting
- Silicon sensor : 500 µm thickness.
- 125 x 75 mm^2 : detector size
- 130 x 130 μm^2 : pixel size
- 560 x 960 pixels
- Fast readout and data transfer : up to 200 frames/s (optical fibre and PCIExpress)

Chips 1x1cm assembled in barrettes,
barrettes assembled in tiles.

Whole-body mouse with spatial resolution of 60 µm

Démonstrateur micro-CT PIXSCAN II

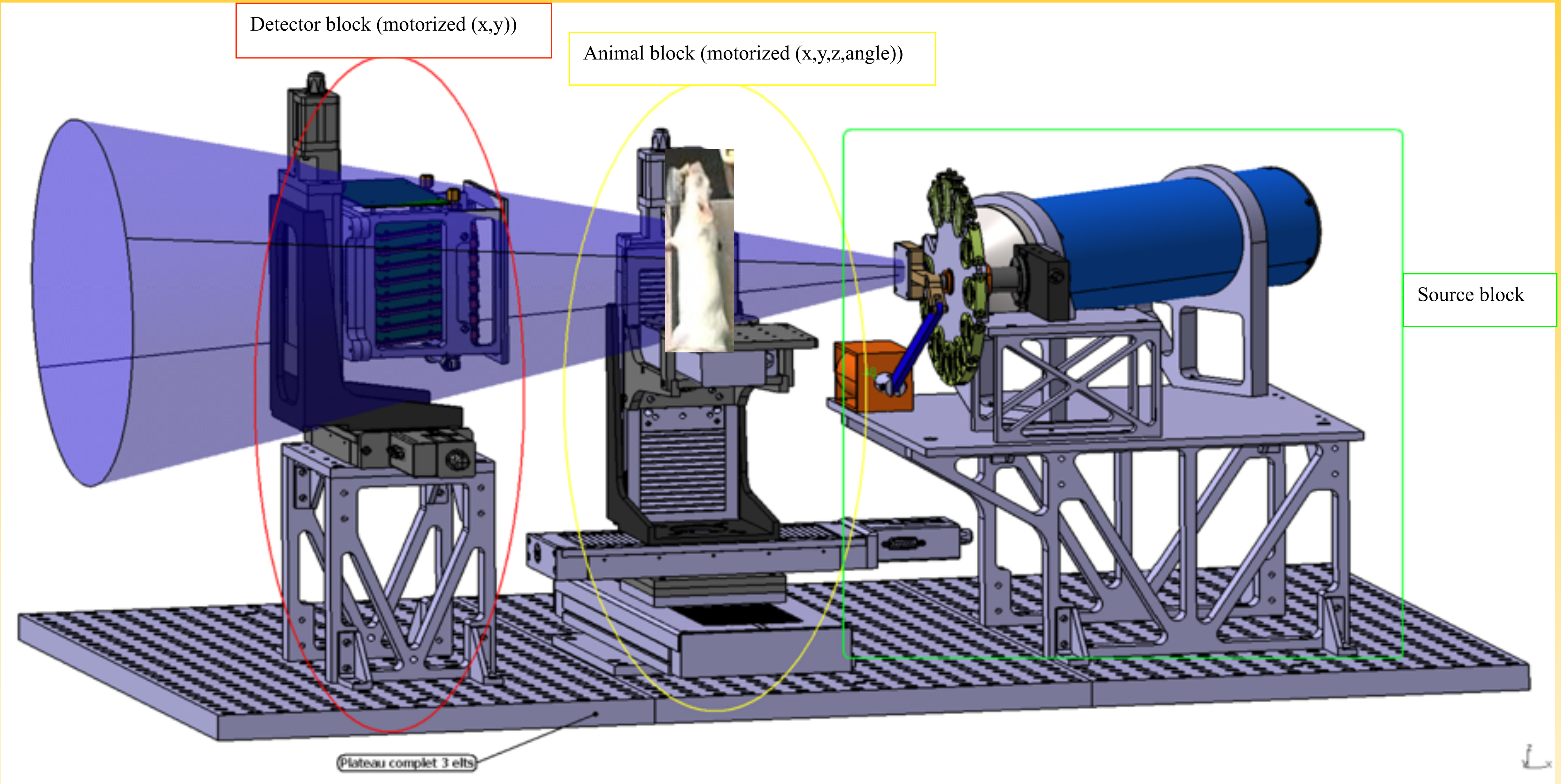

Complete system : 3 blocks

OXFORD Intruments X-ray tube

Target Voltage 10 to 90kv, Target Current up to 2 mA

W target, 13 to 40 µm focal spot size, 80 W, 33 degrees Cone Angle

Démonstrateur micro-CT
PIXSCAN II

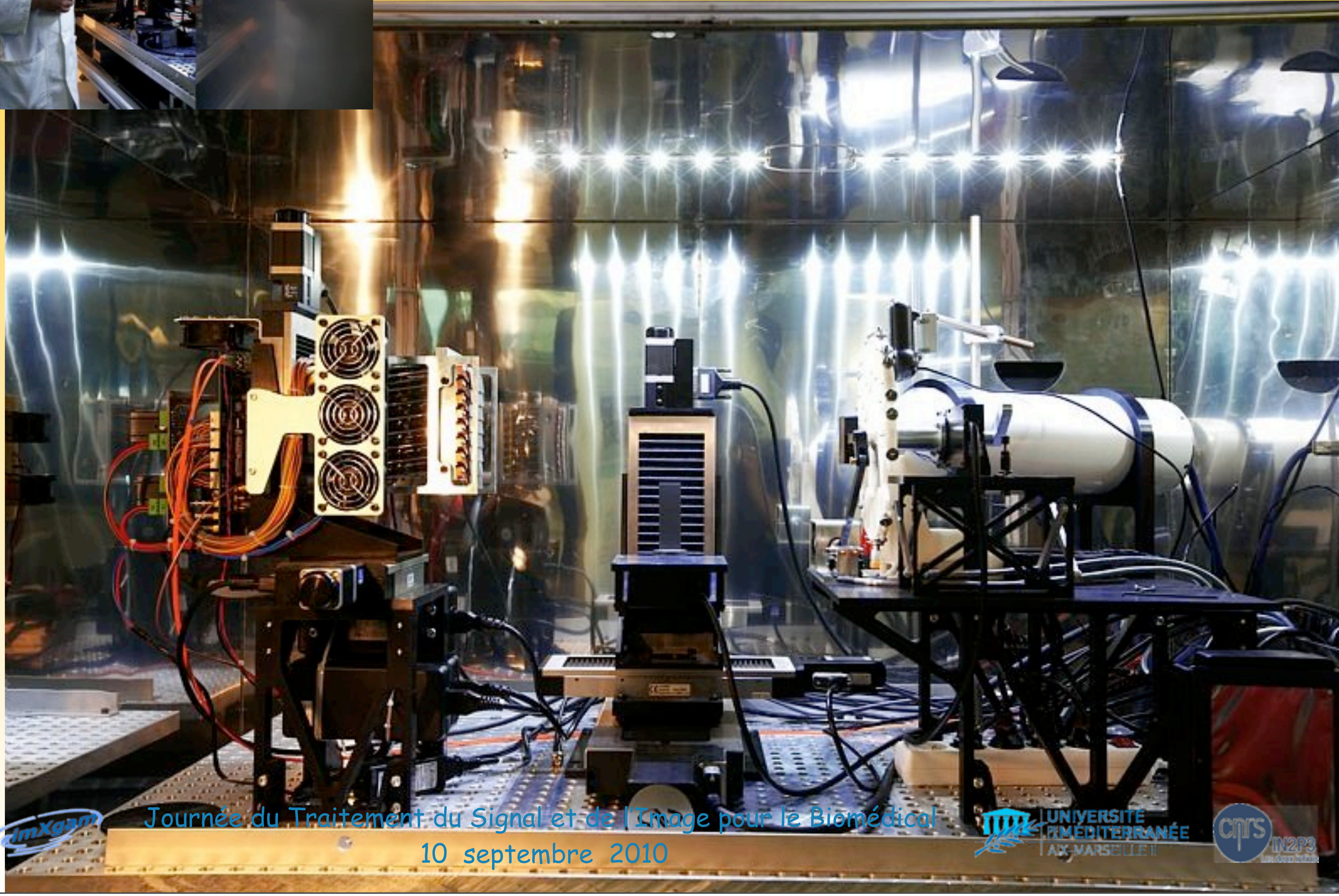

II - Tomography reconstruction

- Basis of tomography : data in 1D + angle, object in 2D.

Image to reconstruct

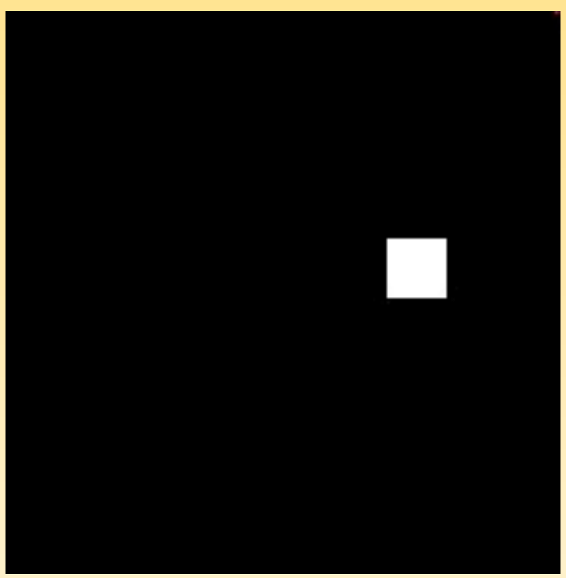

II - Tomography reconstruction

- Basis of tomography : data in 1D + angle, object in 2D.

Image to reconstruct

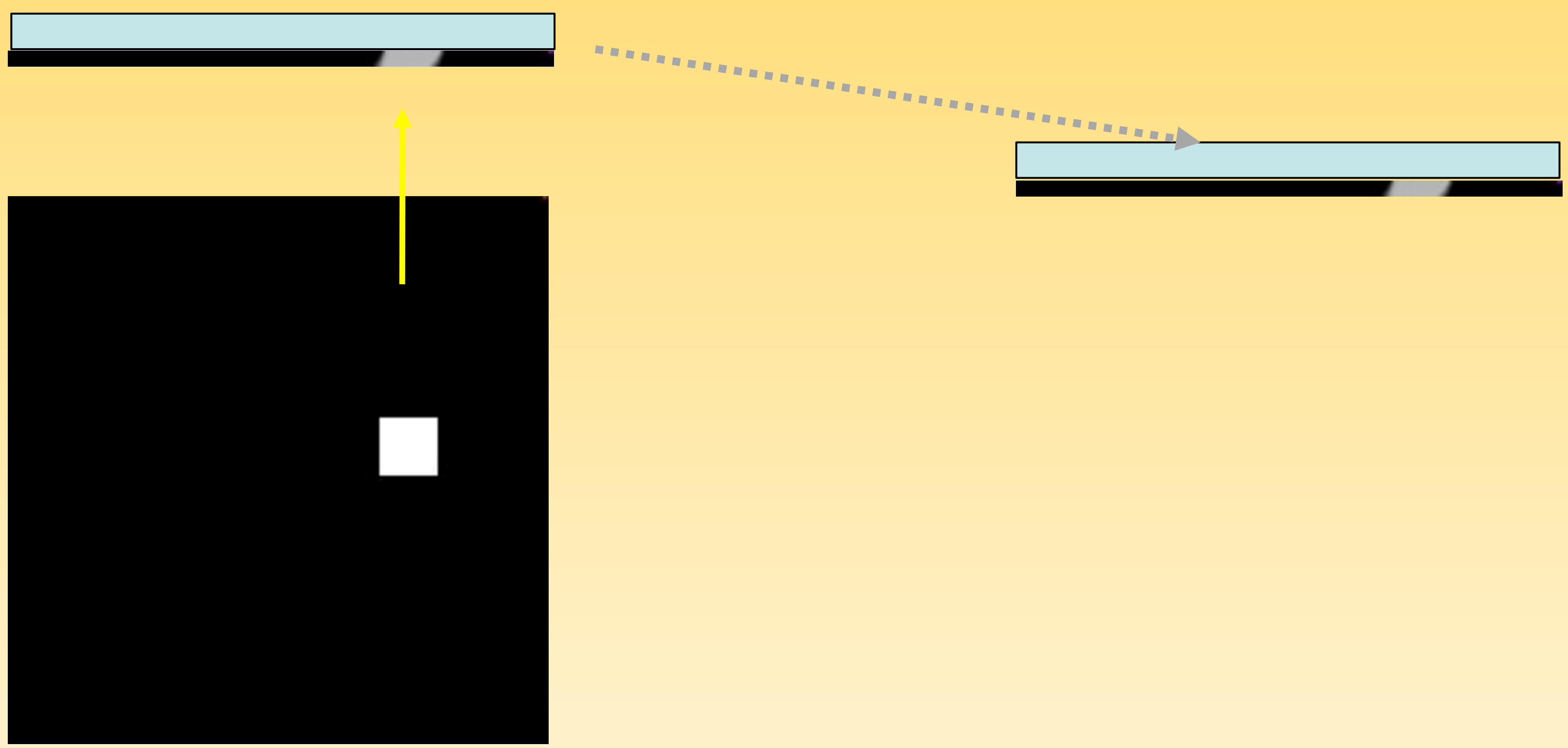

II - Tomography reconstruction

- Basis of tomography : data in 1D + angle, object in 2D.

Image to reconstruct

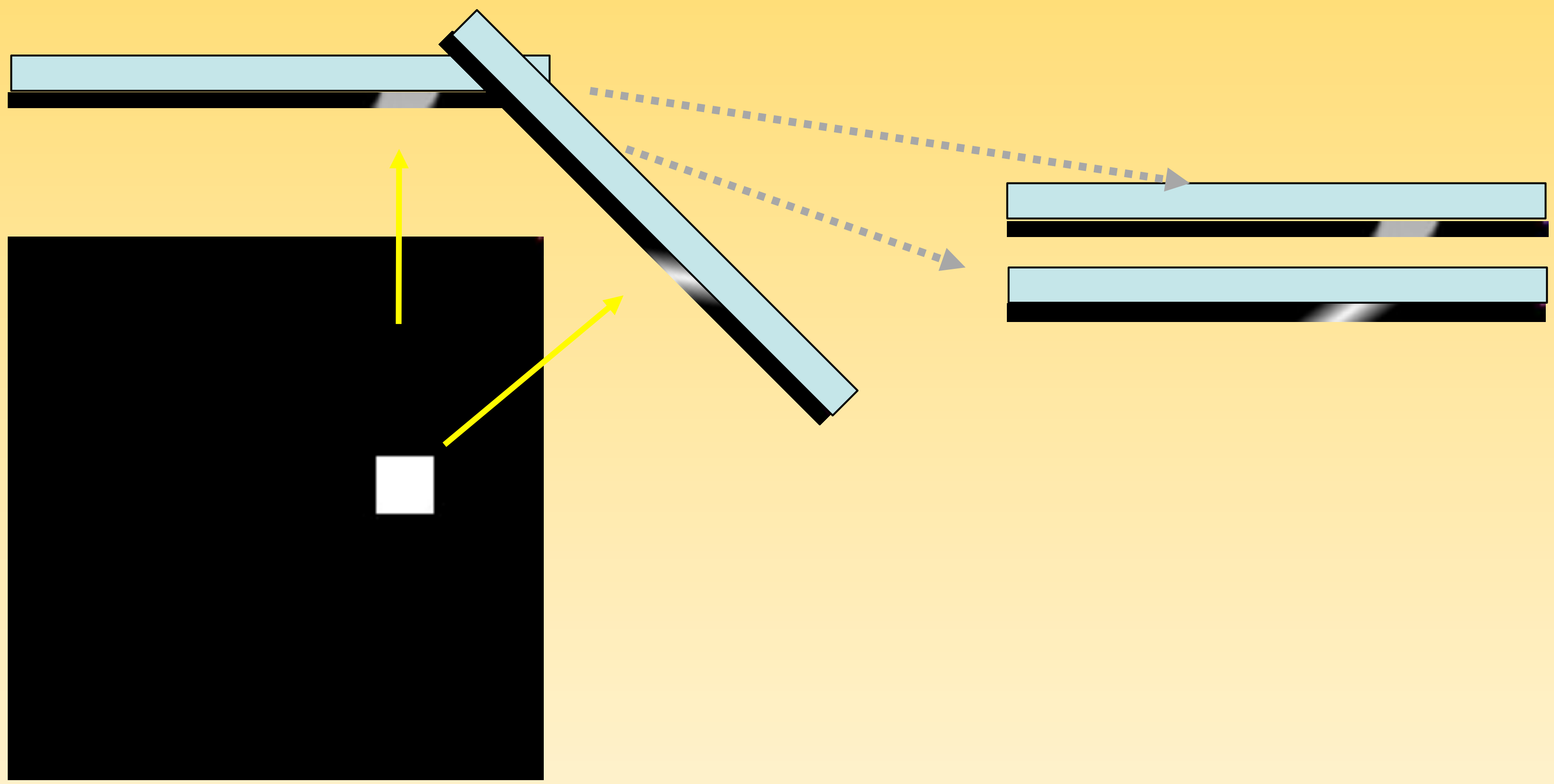

II - Tomography reconstruction

- Basis of tomography : data in 1D + angle, object in 2D.

Image to reconstruct

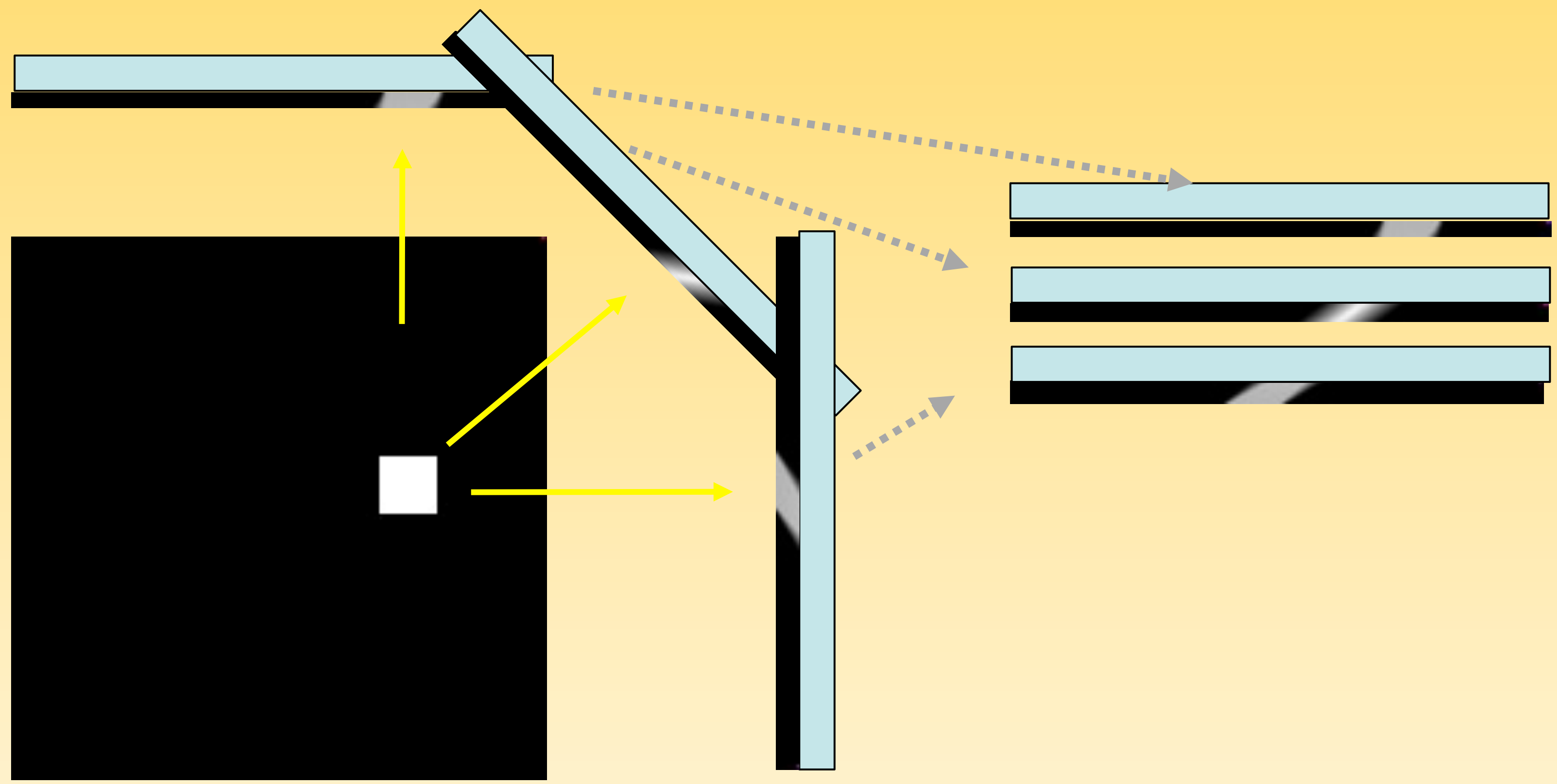

II - Tomography reconstruction

- Basis of tomography : data in 1D + angle, object in 2D.

Image to reconstruct

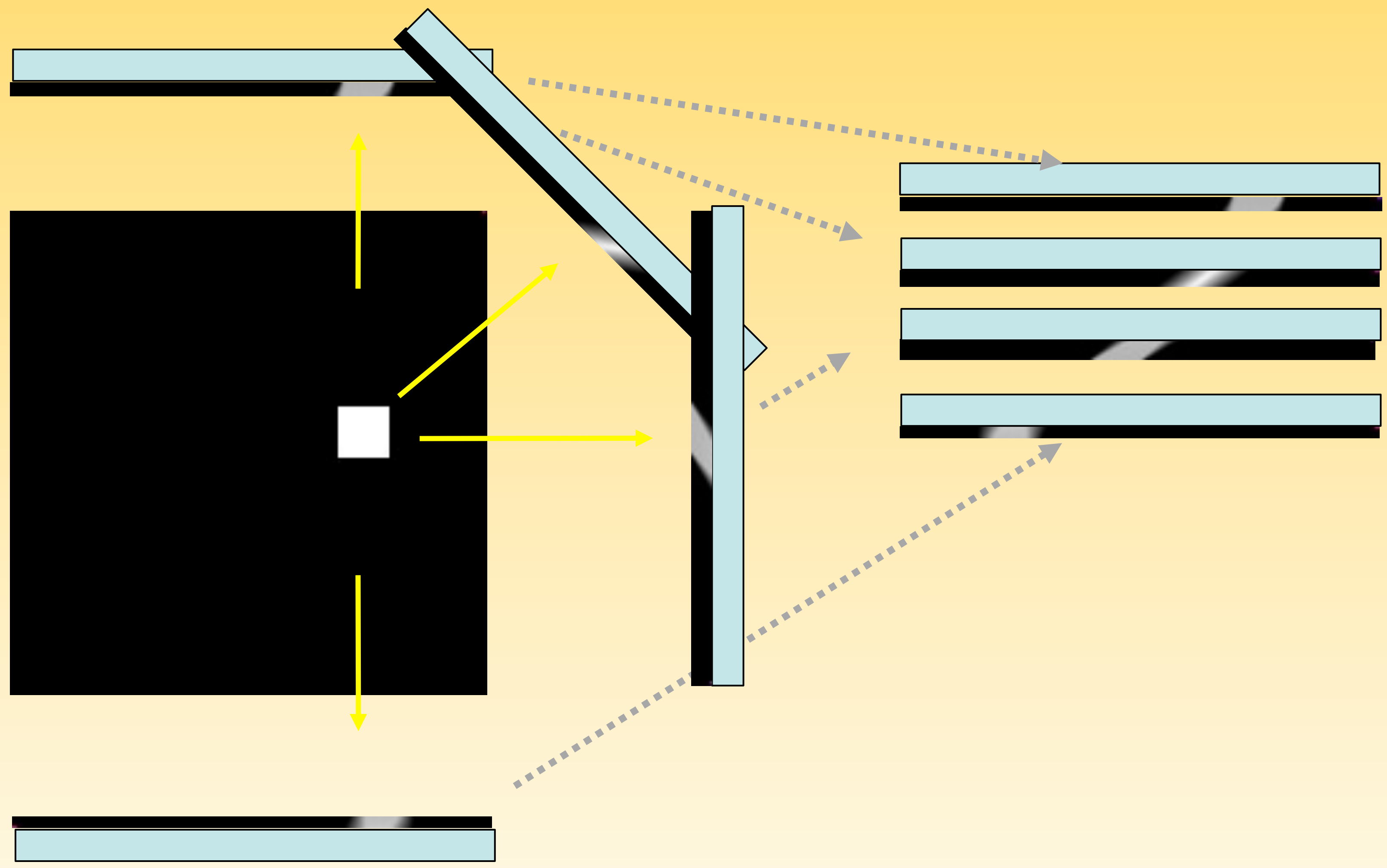

II - Tomography reconstruction

- Basis of tomography : data in 1D + angle, object in 2D.

Image to reconstruct

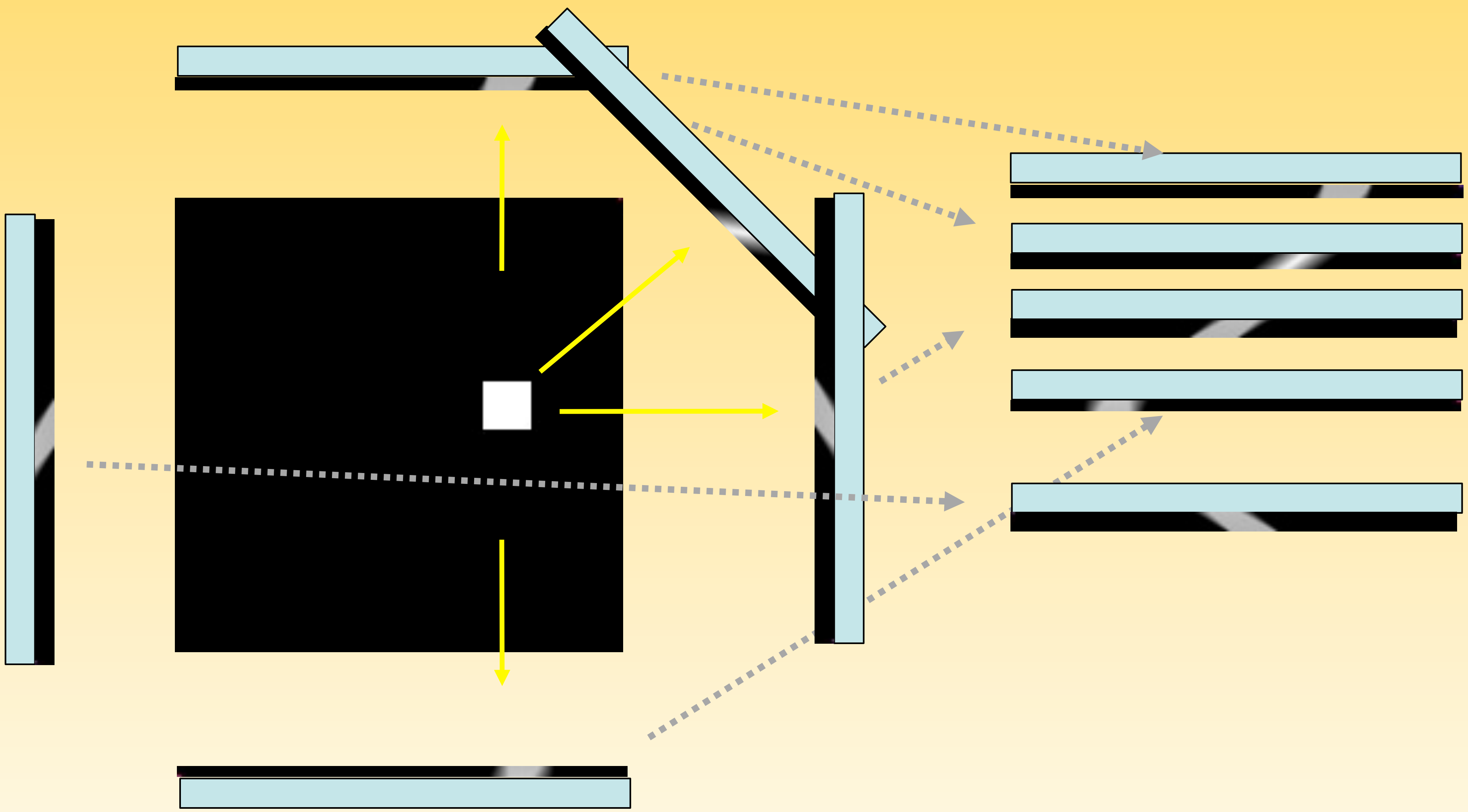

II - Tomography reconstruction

- Basis of tomography : data in 1D + angle, object in 2D.

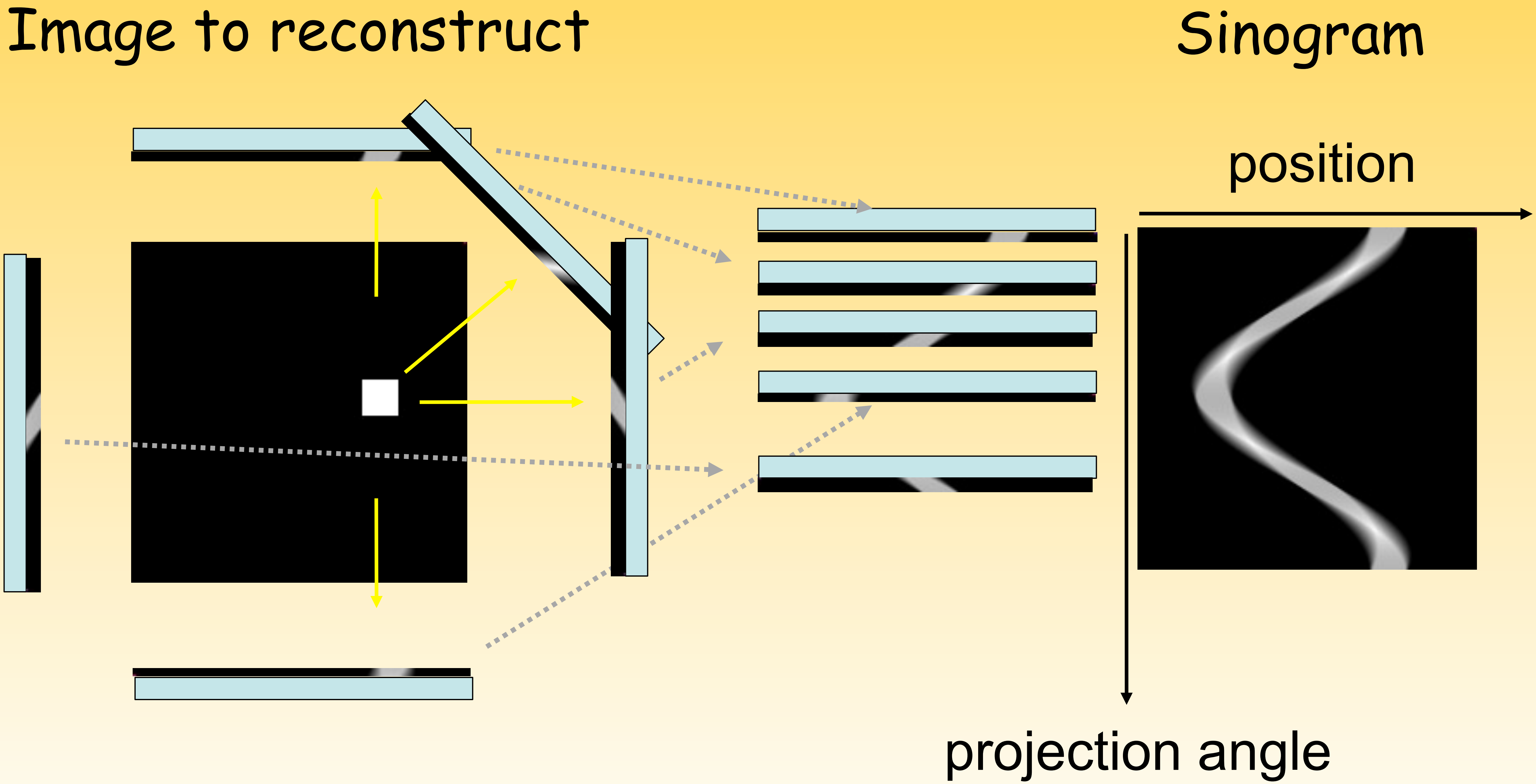

II - Tomography reconstruction

- Basis of tomography : data in 2D + angle, object in 3D.

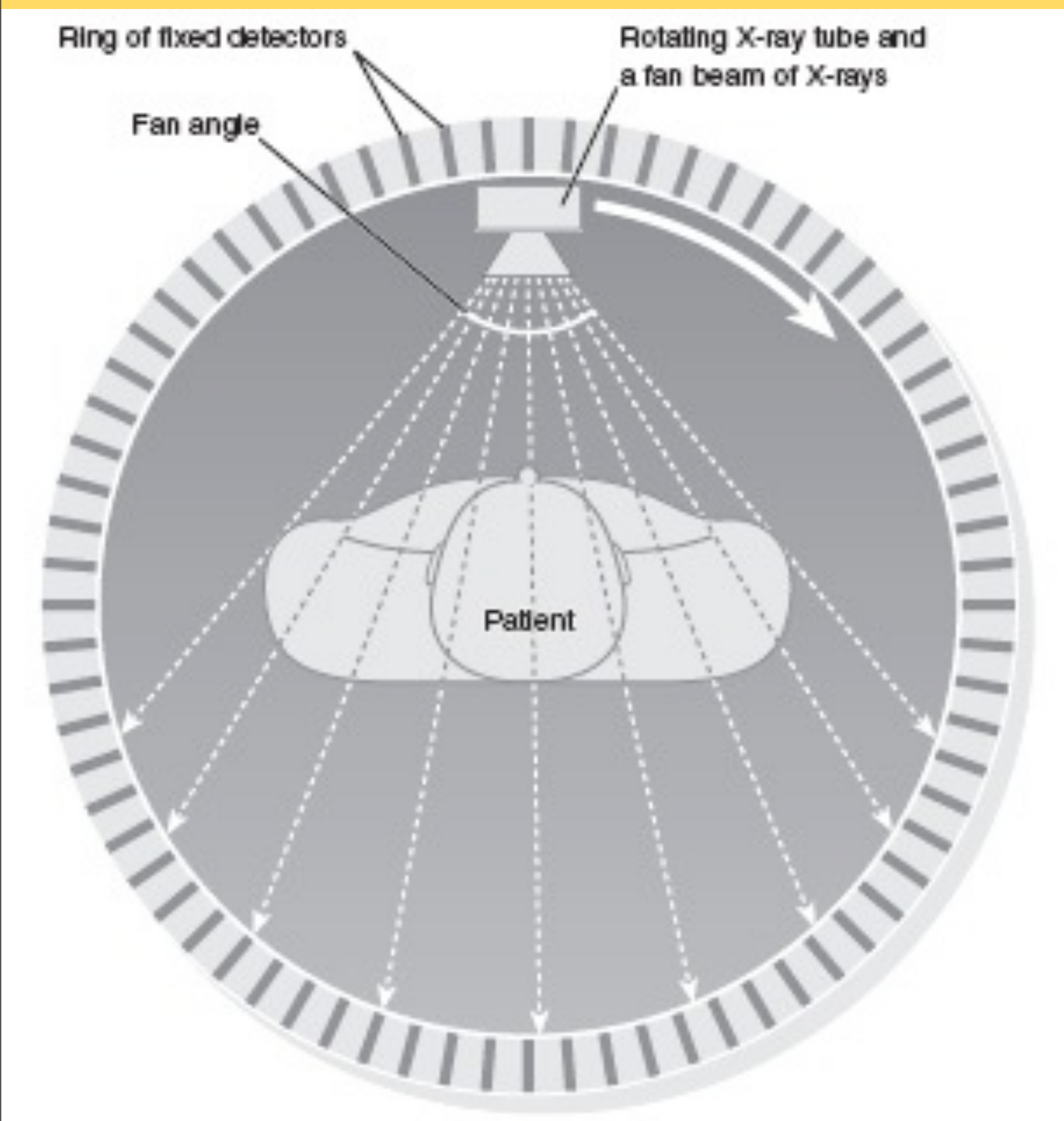

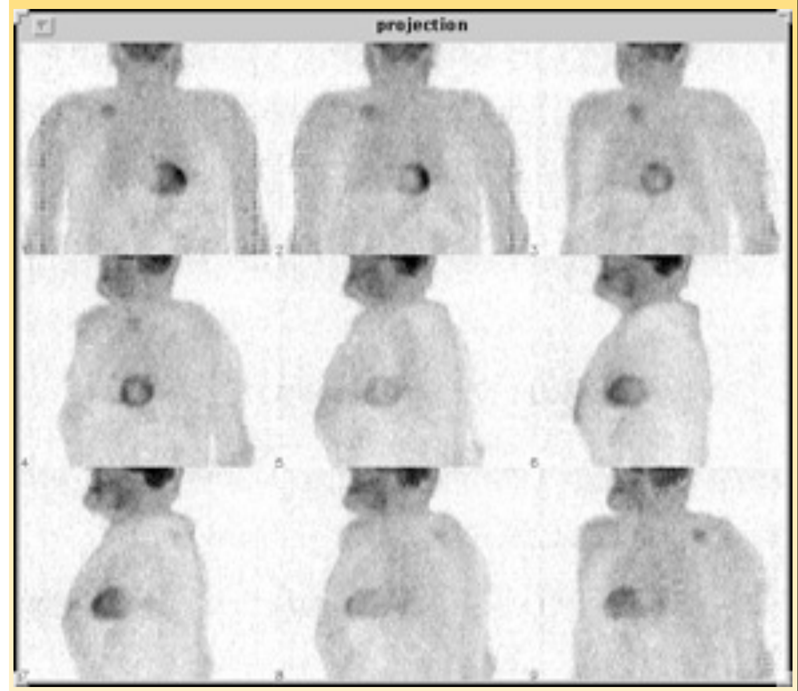

Sinogram

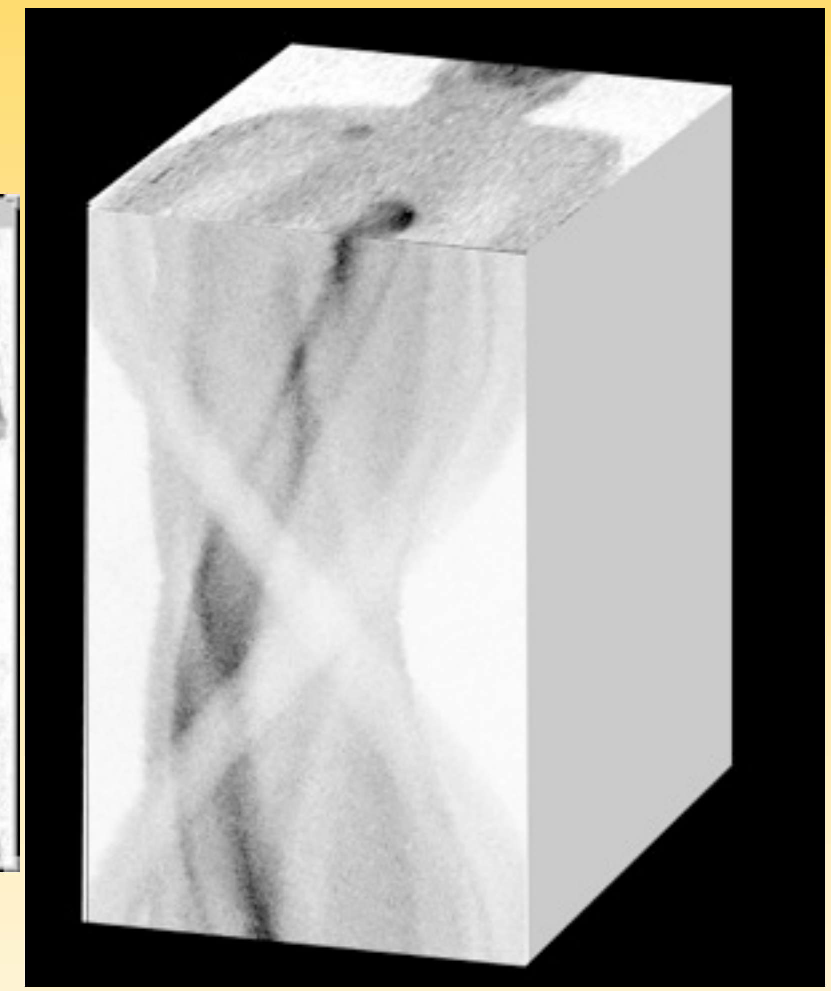

II - Tomography reconstruction

- Basis of tomography : data in 2D + angle, object in 3D.

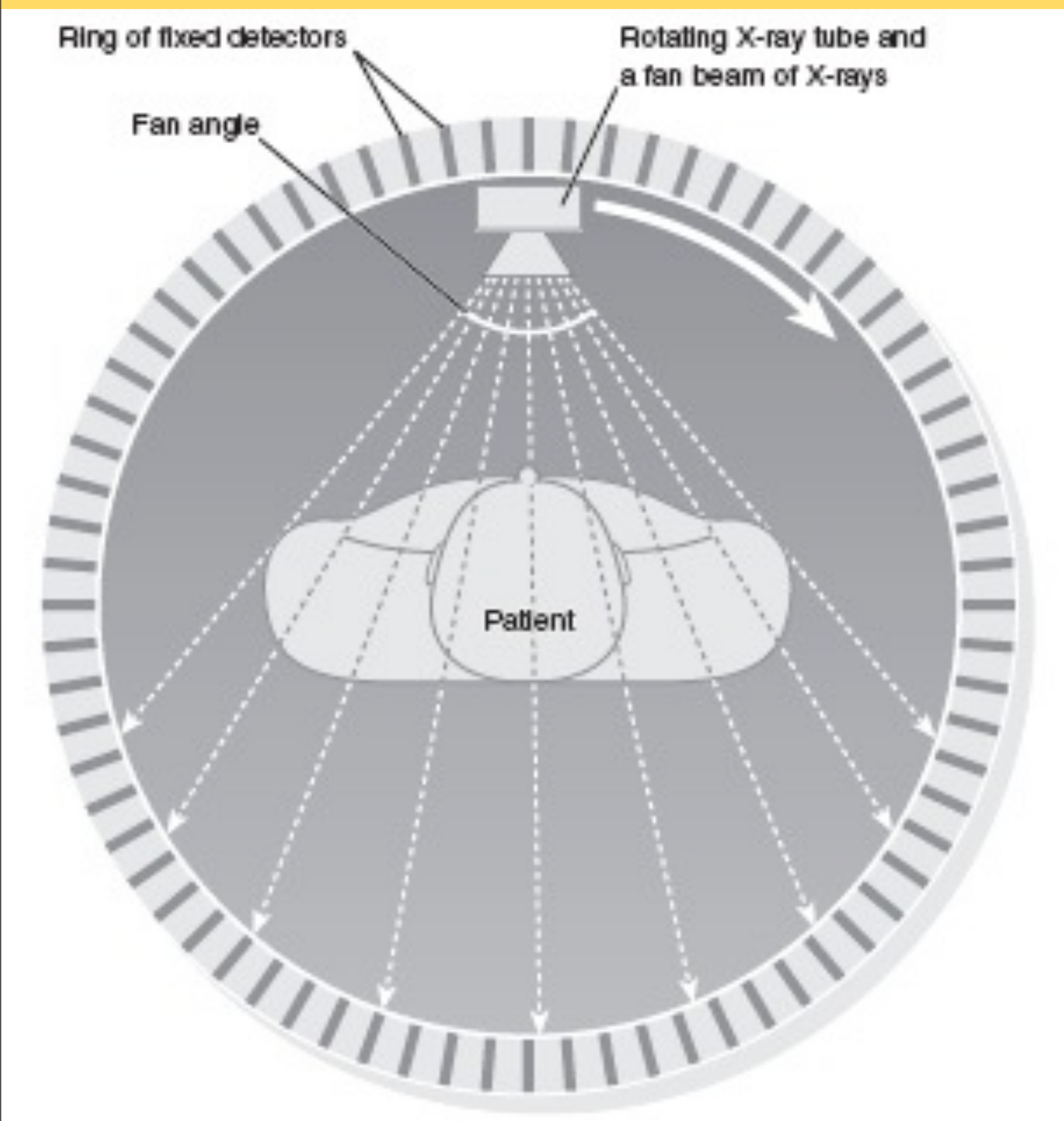

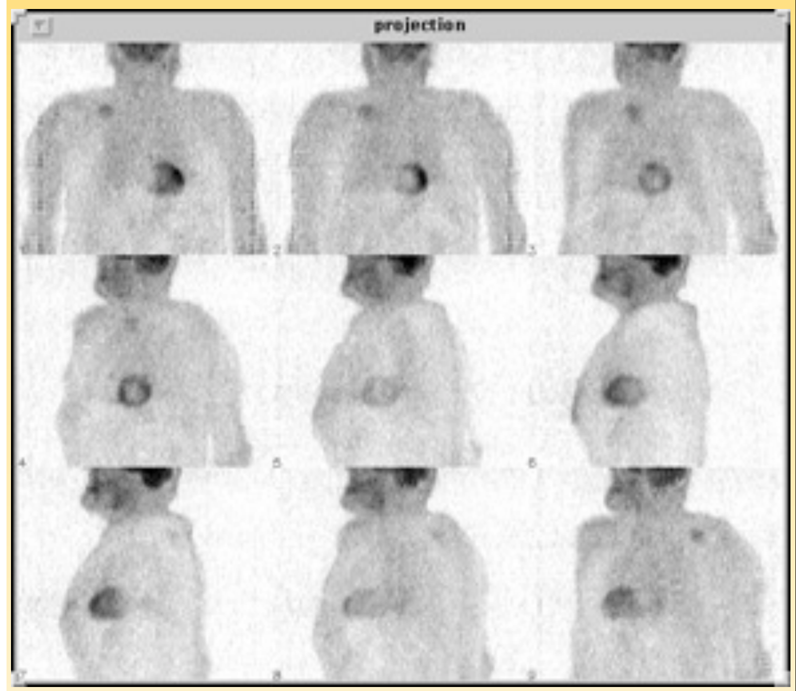

Sinogram

Geometry and physics of the problem

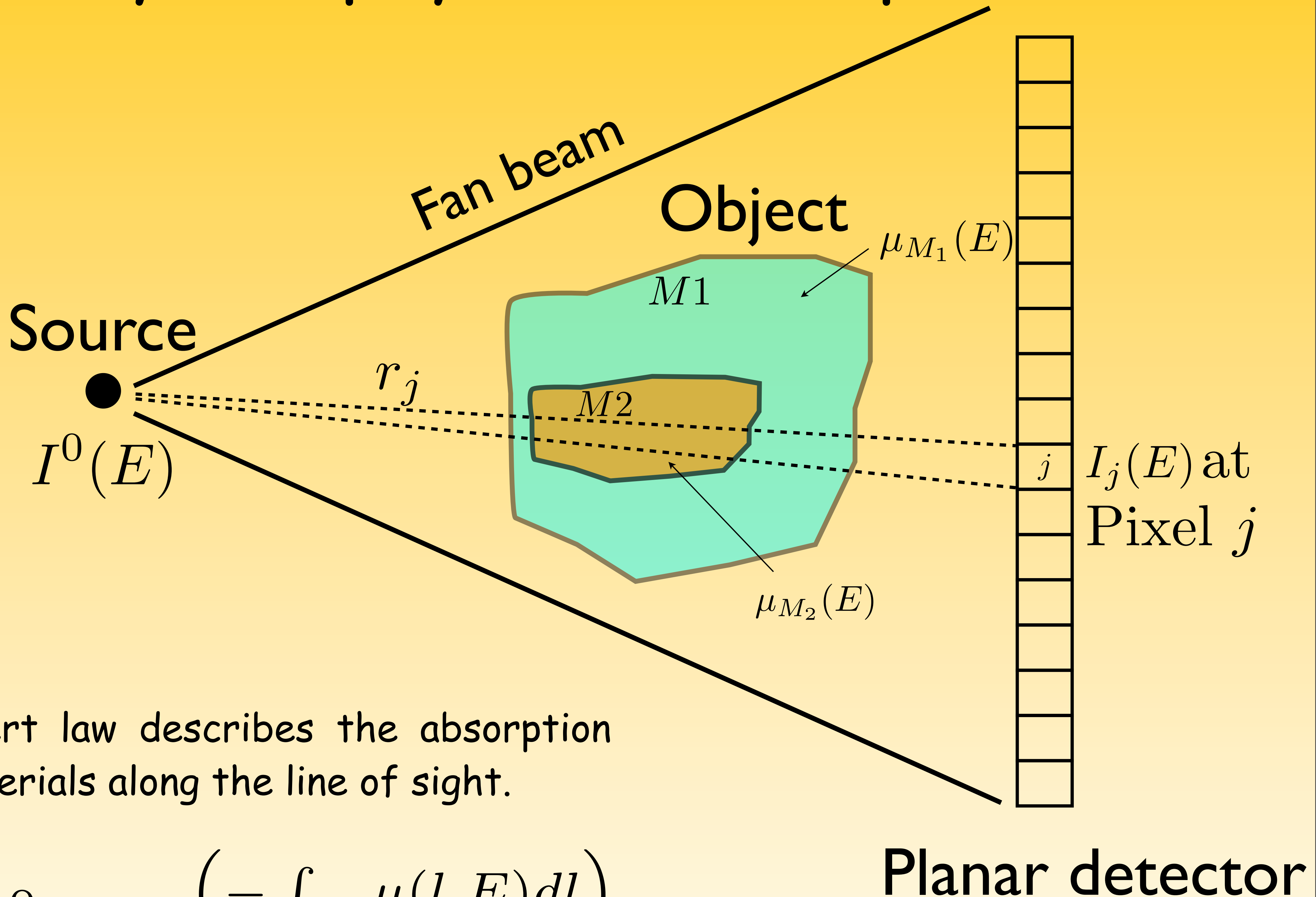

The Beer-Lambert law describes the absorption of different materials along the line of sight.

$$I_j(E) = I^0(E)e^{\left(-\int_{r_j} \mu(l,E)dl\right)}$$

Geometry and physics of the problem

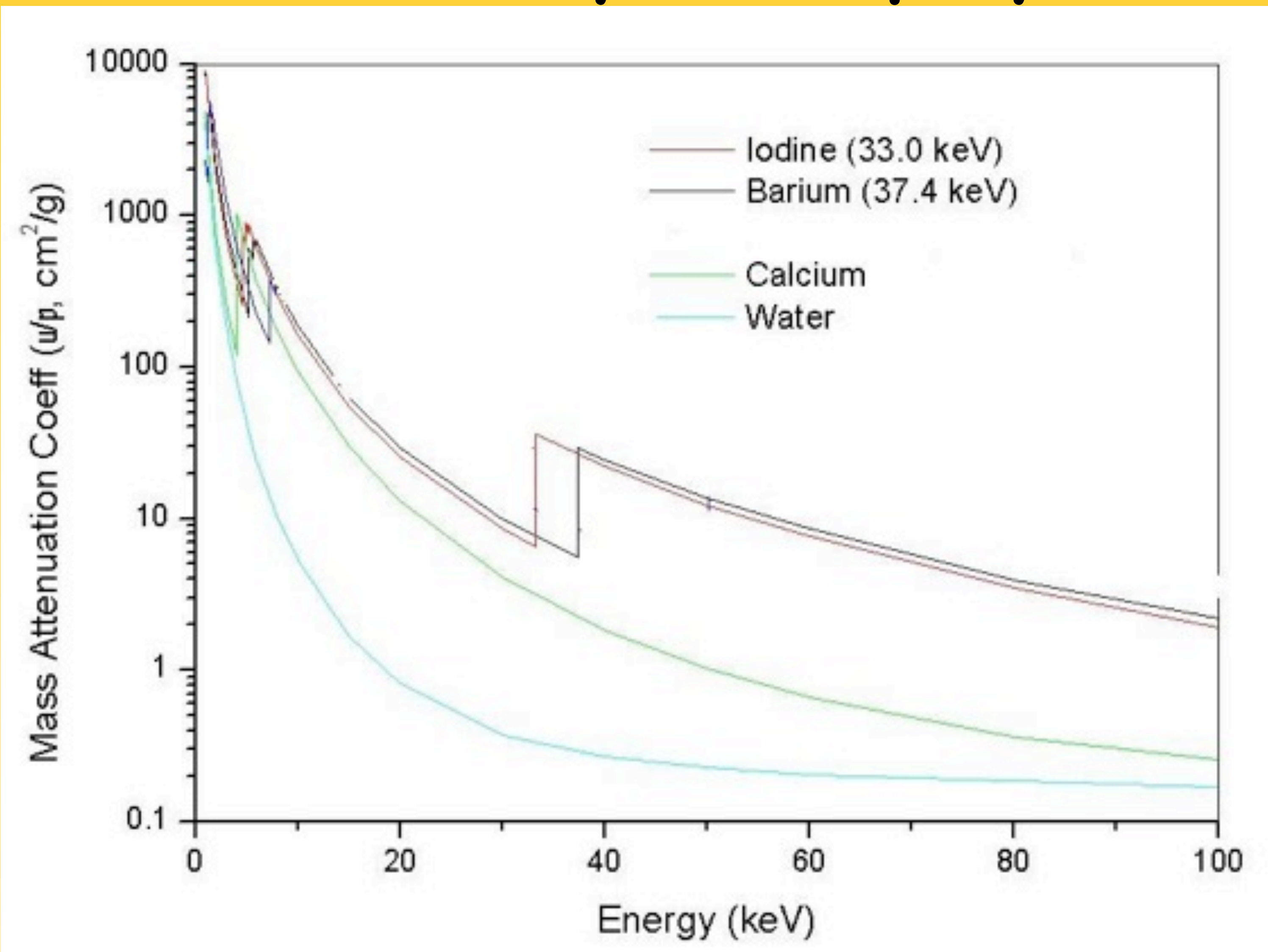

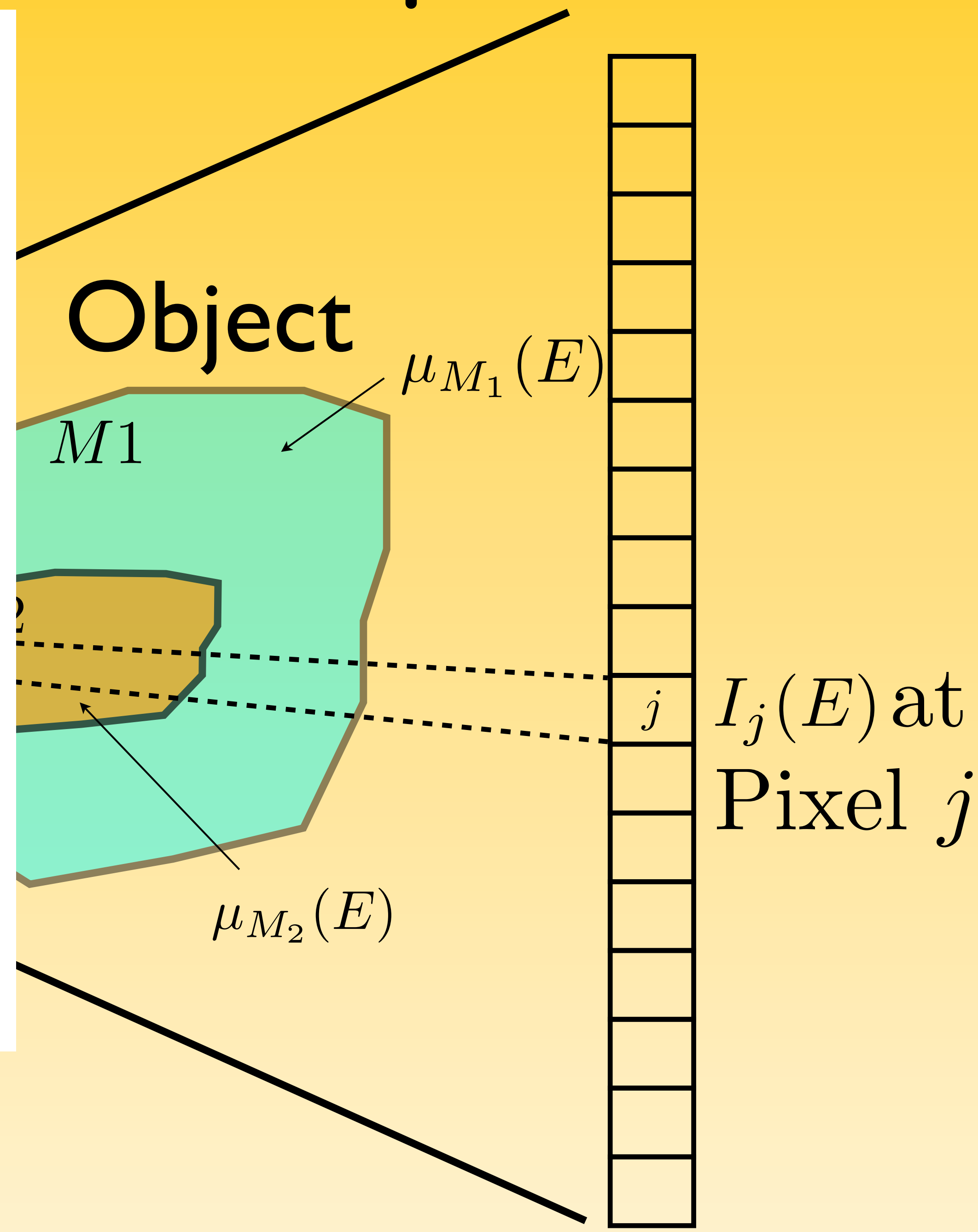

Planar detector

The Beer-Lambert law describes the absorption of different materials along the line of sight.

$$I_j(E) = I^0(E)e^{\left(-\int_{r_j}\mu(l,E)dl\right)}$$

Geometry and physics of the problem

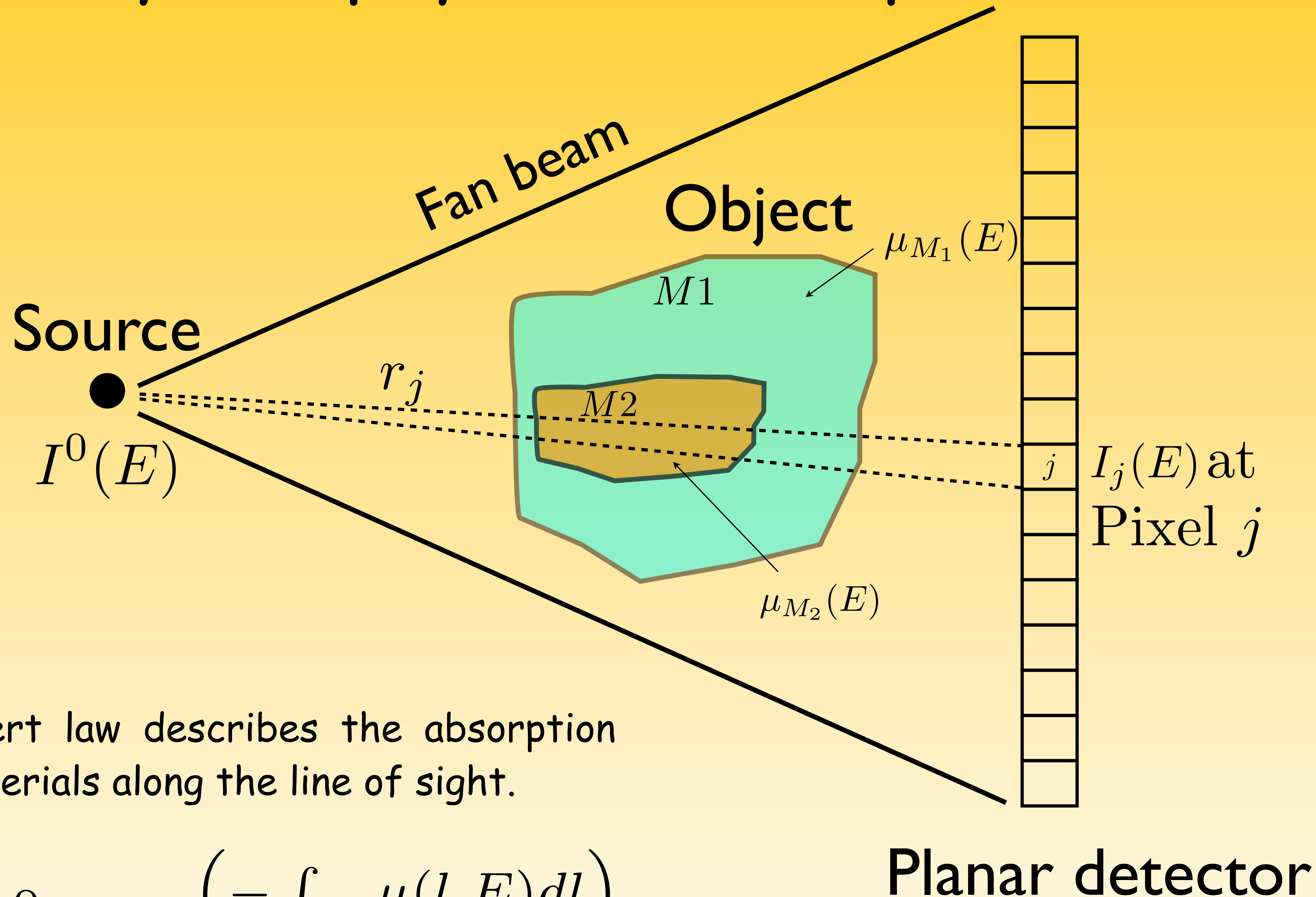

The Beer-Lambert law describes the absorption of different materials along the line of sight.

$$I_j(E) = I^0(E) e^{\left(-\int_{r_j} \mu(l,E) dl\right)}$$

Geometry and physics of the problem

A pixel hybrid will measure $y_{j,T} = \int_{T}^{\infty} I_j(E)dE$

Under the assumption of a monochromatic beam, we get at energy E_0

$$y_{j,T} = I^0(E_0)e^{-\int_{r_j} \mu(l,E_0)dl}$$

so that $\ln\left(\frac{y_{j,T}}{I^0(E_0)}\right) = -\int_{r_j} \mu(l,E_0)dl$

In a discrete world where the ray r_j cuts all the voxels i, we finally get

$$x_j = \ln\left(\frac{y_{j,T}}{I^0(E_0)}\right) = -\sum_i \alpha_i \mu_i$$

Geometry and physics of the problem

The problem is expressed as a linear problem :

$$X = A\mu$$

where $X = (x_j)_{j\in\mathbb{N}_m}, \in \mathbb{R}^m$ are the measures,

and $\mu = (\mu_i)_{i\in\mathbb{N}_n}, \in \mathbb{R}^n$ is the attenuation vector to recover

and $A = (\alpha_{i,j})_{(i,j)\in\mathbb{N}_n\times\mathbb{N}_m}$ is the matrix system.

with $n > m$ in general ...

Realistic model incorporating Poisson noise :

$$X = \mathcal{P}(A\mu)$$

Geometry and physics of the problem

State of the art in tomography :

- Filtered Back-Projection based algorithms.

- «Algebraic» Iterative Methods solving a L_2 problem :

$$\hat{\mu} = \arg\min_{\mu} \|X - A\mu\|_2$$

- «Statistical» Iterative Methods incorporating the Poisson noise :

$$\hat{\mu} = \arg\max_{\mu} f(\mu|X) = \arg\max_{\mu} f(X|\mu) f_p(\mu)$$

where $f(\mu|X)$ is the log-likelihood.

First light XPAD3/PIXSCAN II

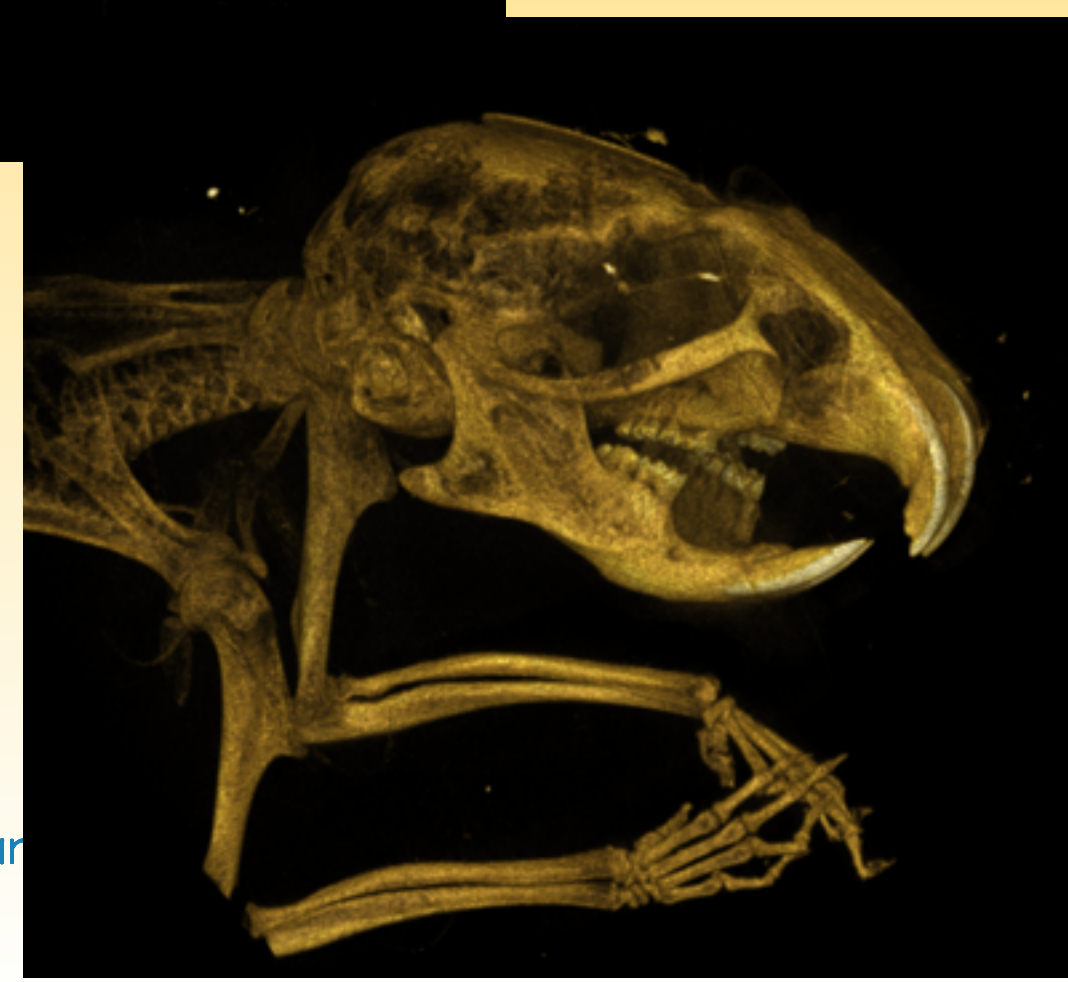

Reconstruction performed on a GPU AMD/ATI, Algorithm FDK.

But need of 720 projections and >1mGy/s at 160 mm

III - Future challenges

1 - Reducing the dose may mean :

- Reducing the statistics
- Reducing the number of projections

→ Need to add a priori information

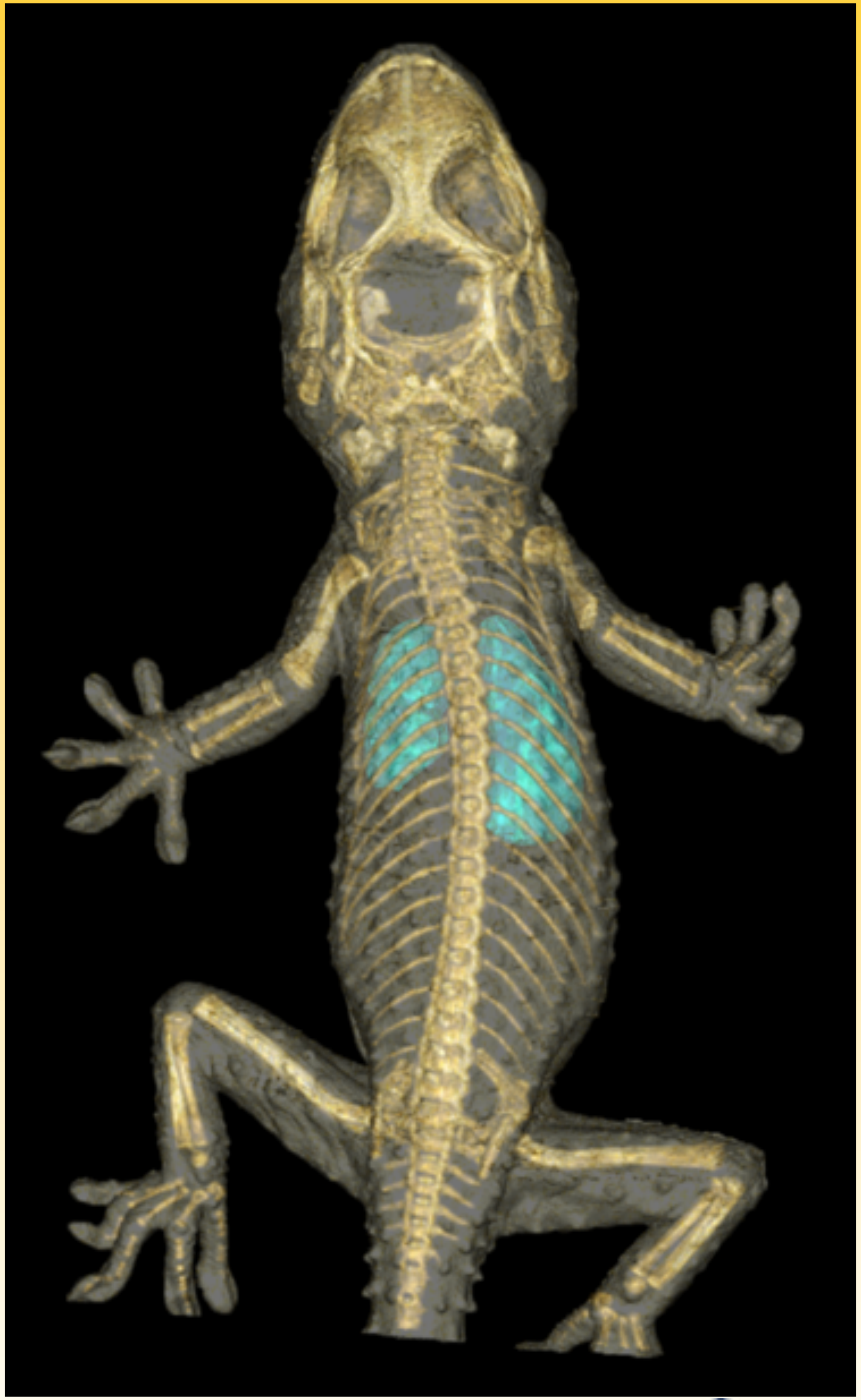

2 - Go towards color imaging !

- Energy selection ! ..
- Acquire directly color information ?

Reducing the statistics

Tests have been performed on a simulated phantom with the software GATE.

openGATE : active collaboration with more than 1000 referenced users.

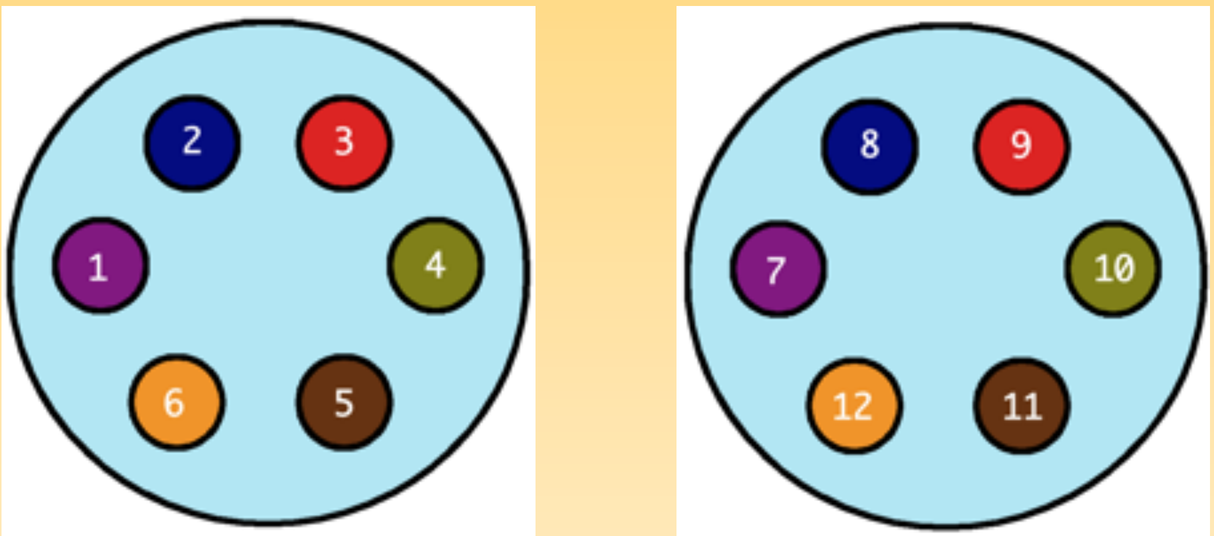

Two horizontal slices of the cylindrical simulated phantom, with different density balls.

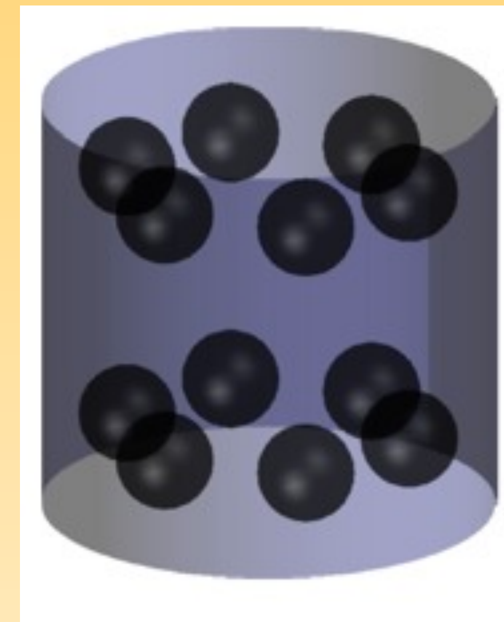

Simulated phantom

Two distinct levels in the phantom with known-density small balls.

Simulations have been performed with :
- Acquired projections of size 100 x 100 pixels, 360 projections.
- A reconstructed volume of 100 x 100 x 100 pixels.
- Activity (Photons/pixels) ranging from 100 to 25600 ph/pix.

Reducing the statistics

Introduction of a priori information in ML-EM algorithm

$$\hat{\mu} = \arg\max_{\mu} \; f(\mu|X) = \arg\max_{\mu} \; f(X|\mu) f_p(\mu)$$

Markov prior based on a median filtering

$$f_p(\mu) = C \exp\left(-\beta U(\mu)\right)$$

$$f_p(\mu_i) = C \exp\left(-\frac{\beta}{2} \sum_b \frac{(\mu_b - m_b)^2}{m_b}\right)$$

Reducing the statistics

ML-EM

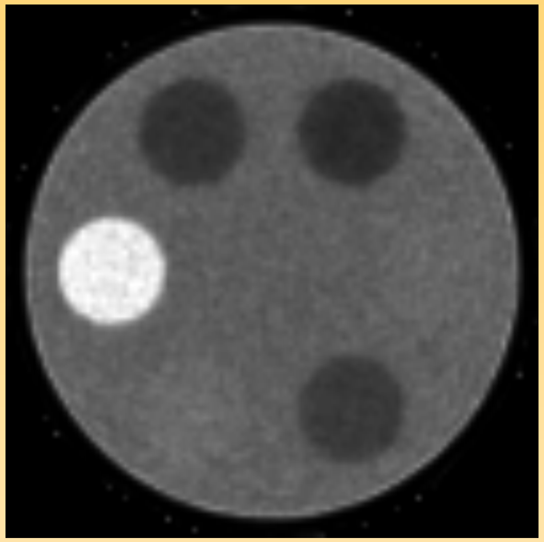

1600 ph/pix

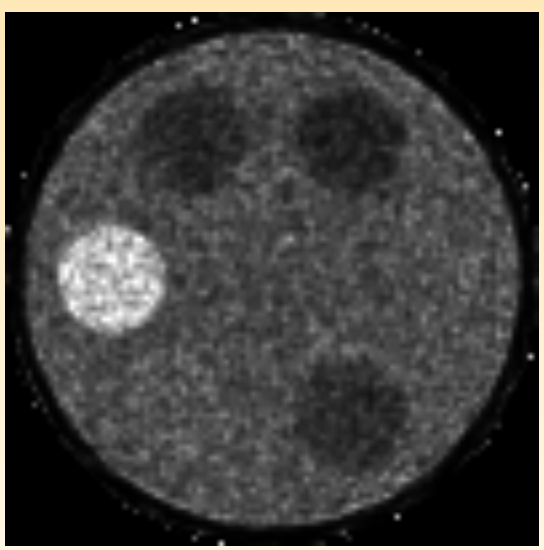

100 ph/pix

Expected volume

Median Root Prior

1600 ph/pix

100 ph/pix

Reducing the statistics

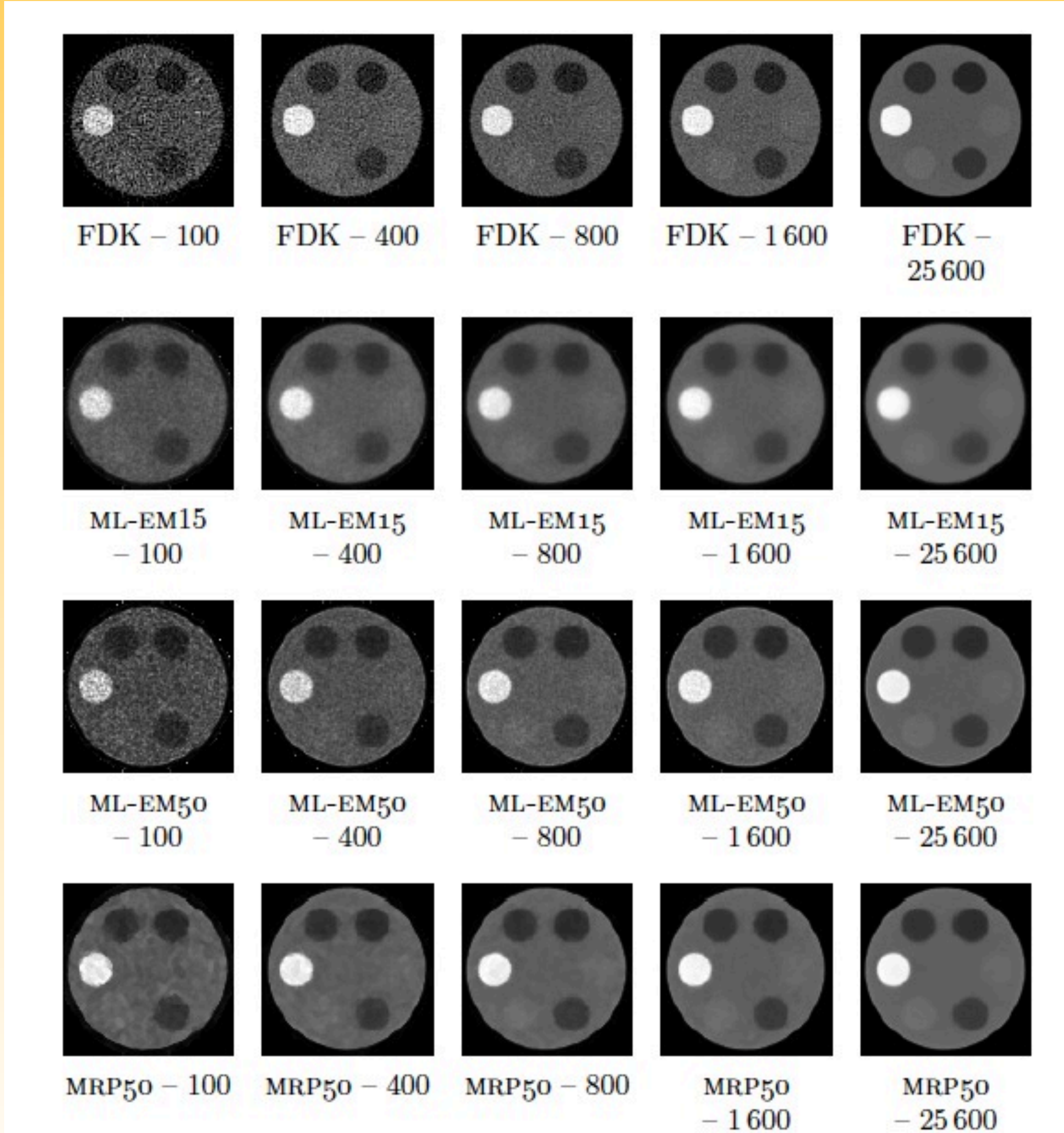

Reducing the statistics

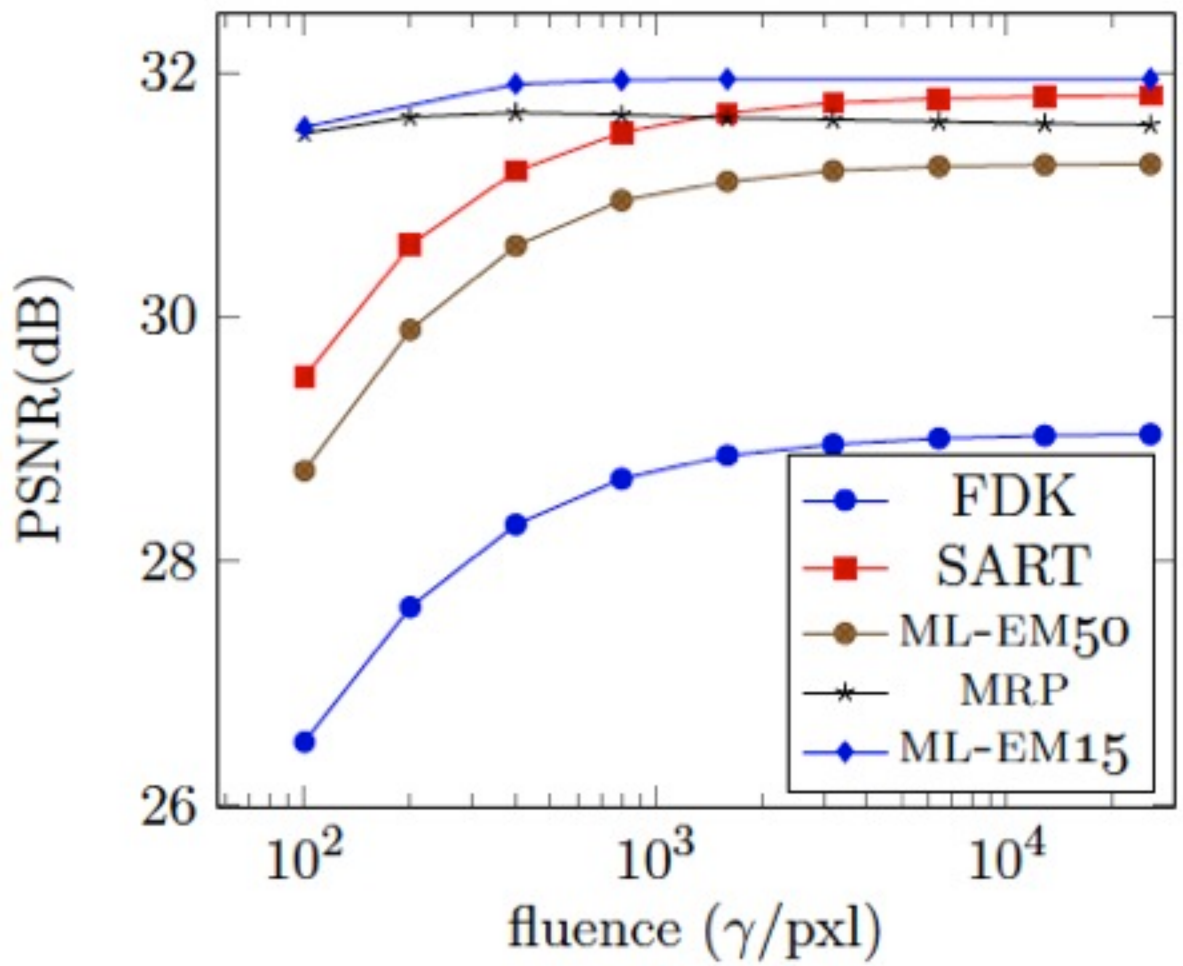

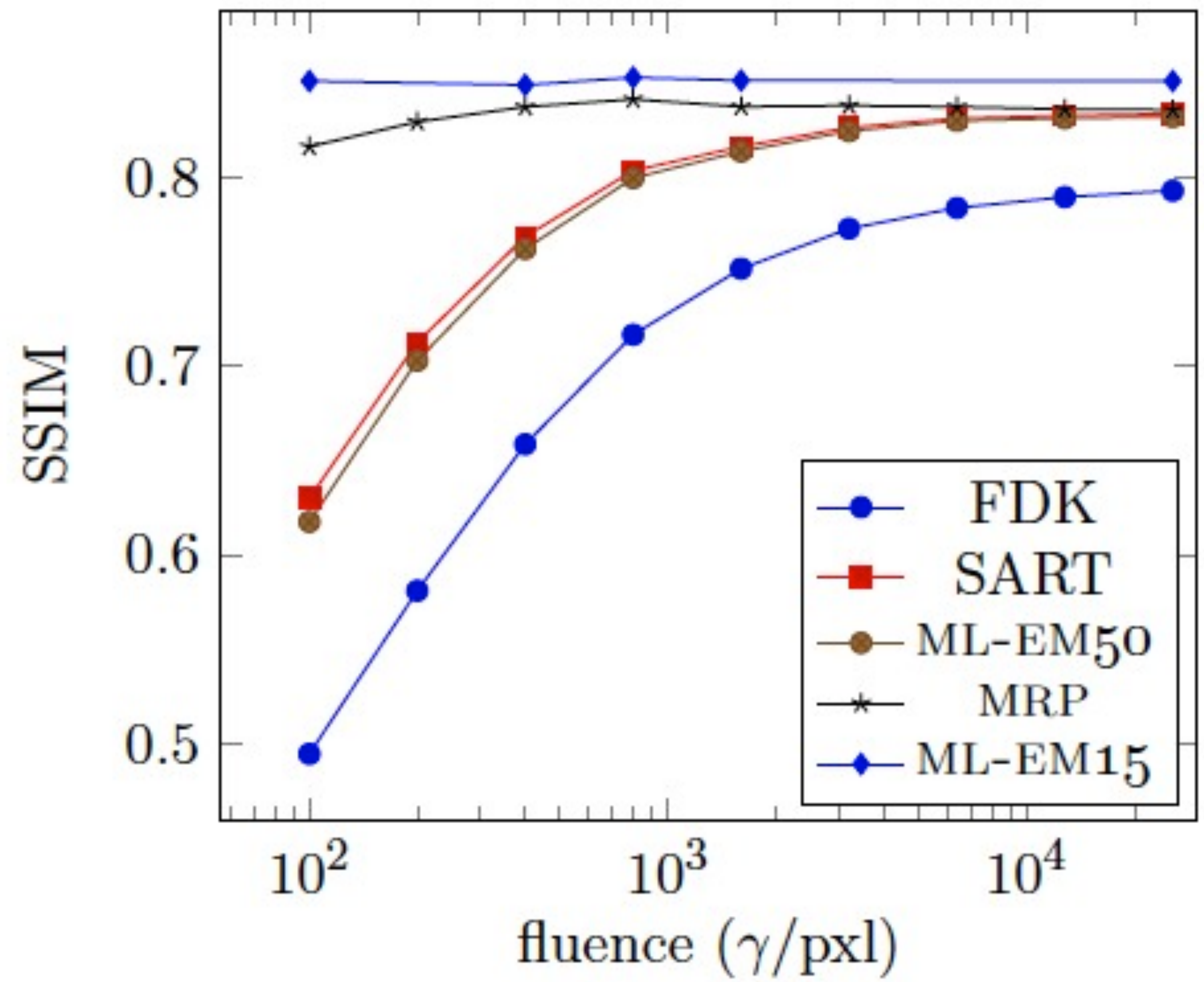

Reducing the number of projections

$$X = A\mu \quad \text{where} \quad A \sim [10^6 - 10^9] \times 10^9$$

Shepp-Logan phantom

Fourier acquisition

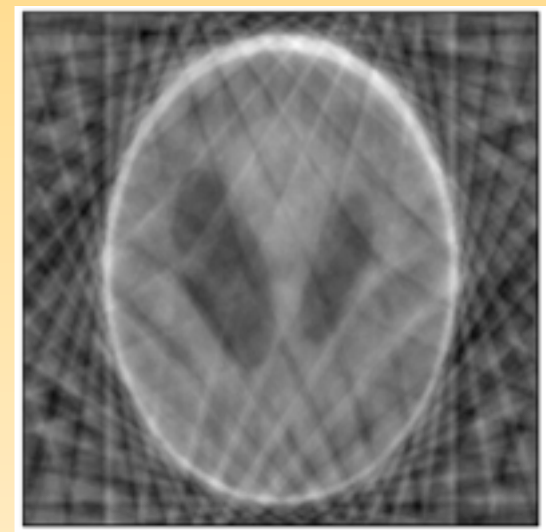

Backprojection

BPDN - TV

BPDN - TV

$$\hat{\mu} = \arg\min_{\mu} \|\mu\|_{TV} \quad \text{s.t.} \quad X = A\mu$$

Reducing the number of projections

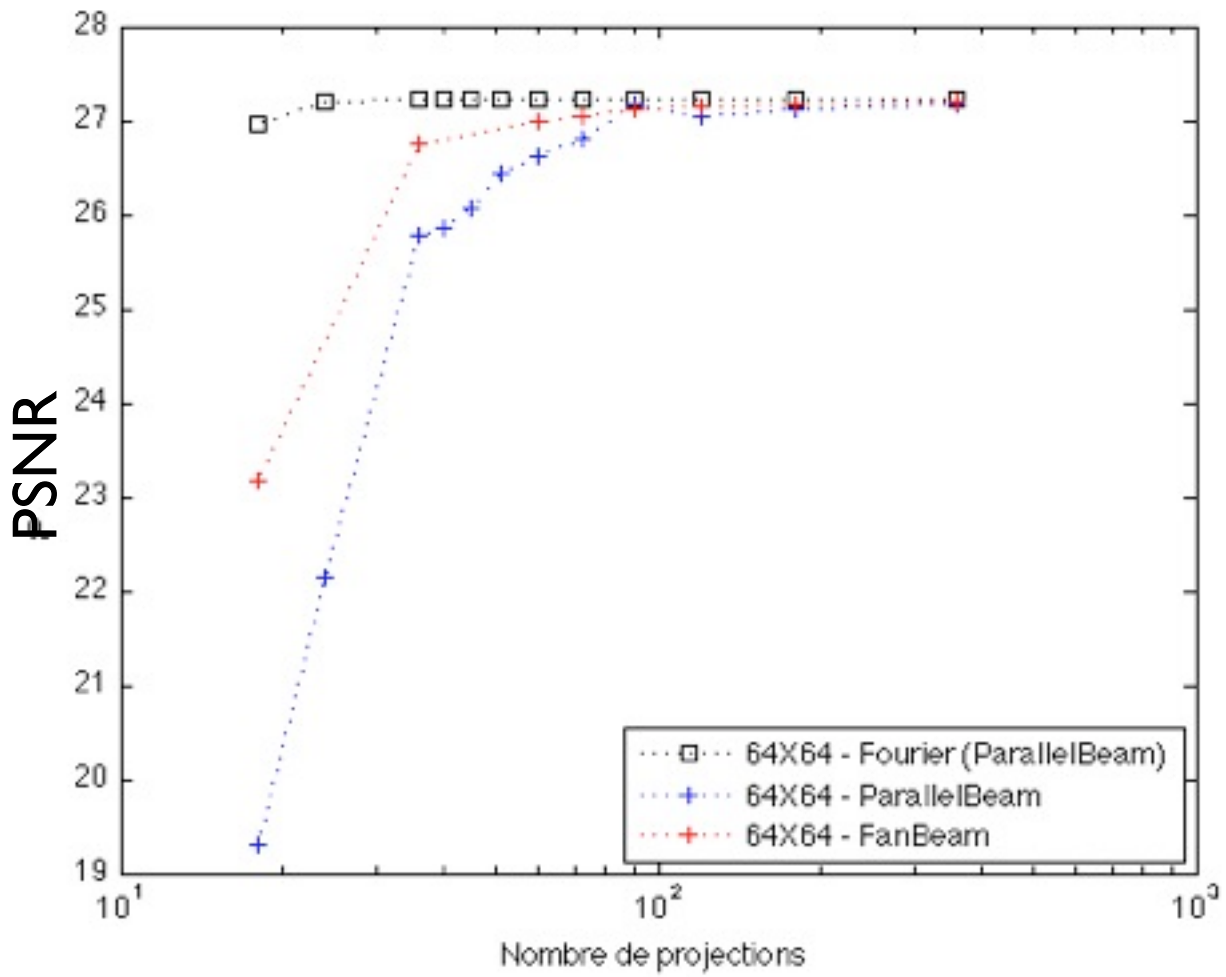

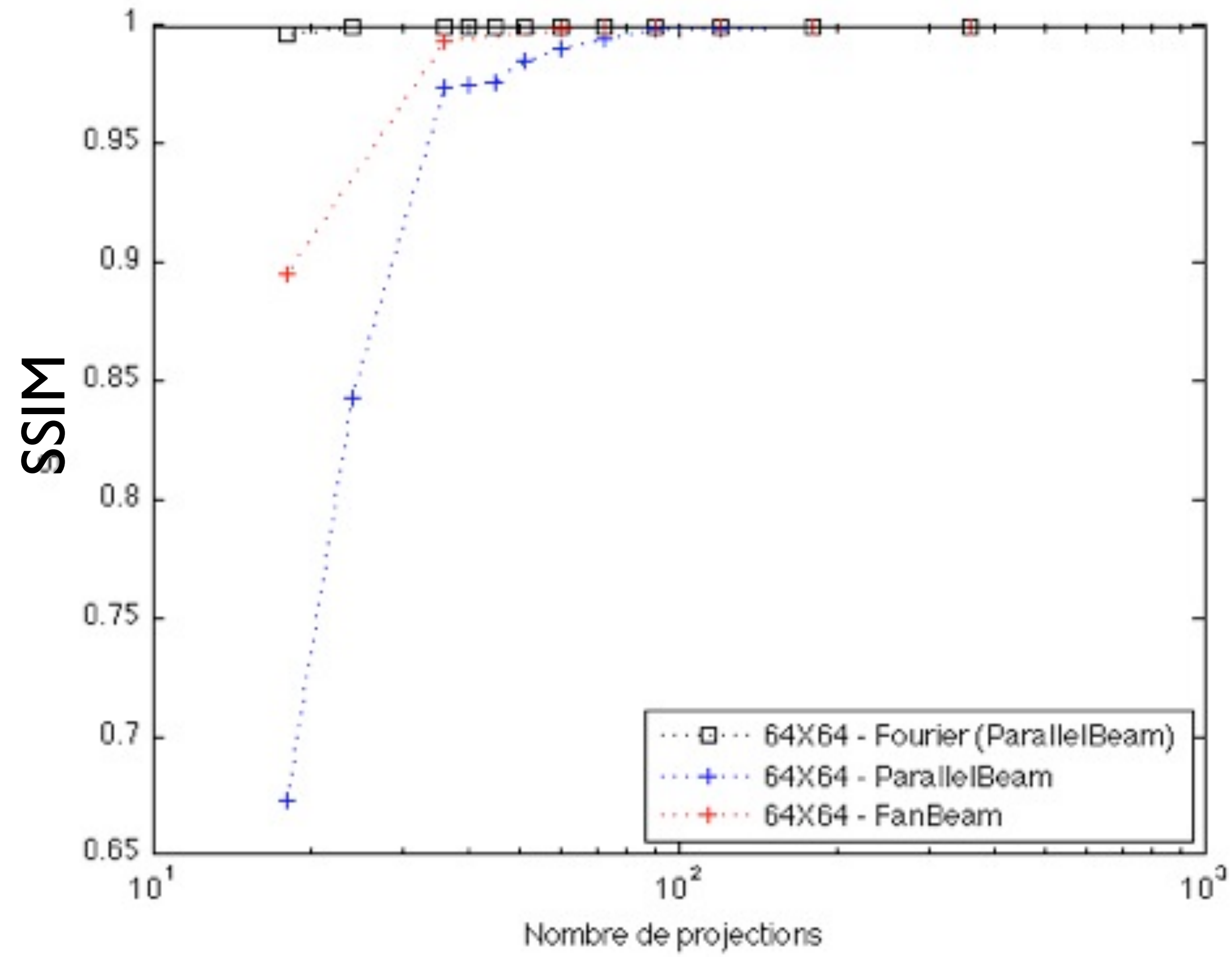

Go towards X-color imaging : concept

Contrast magnification

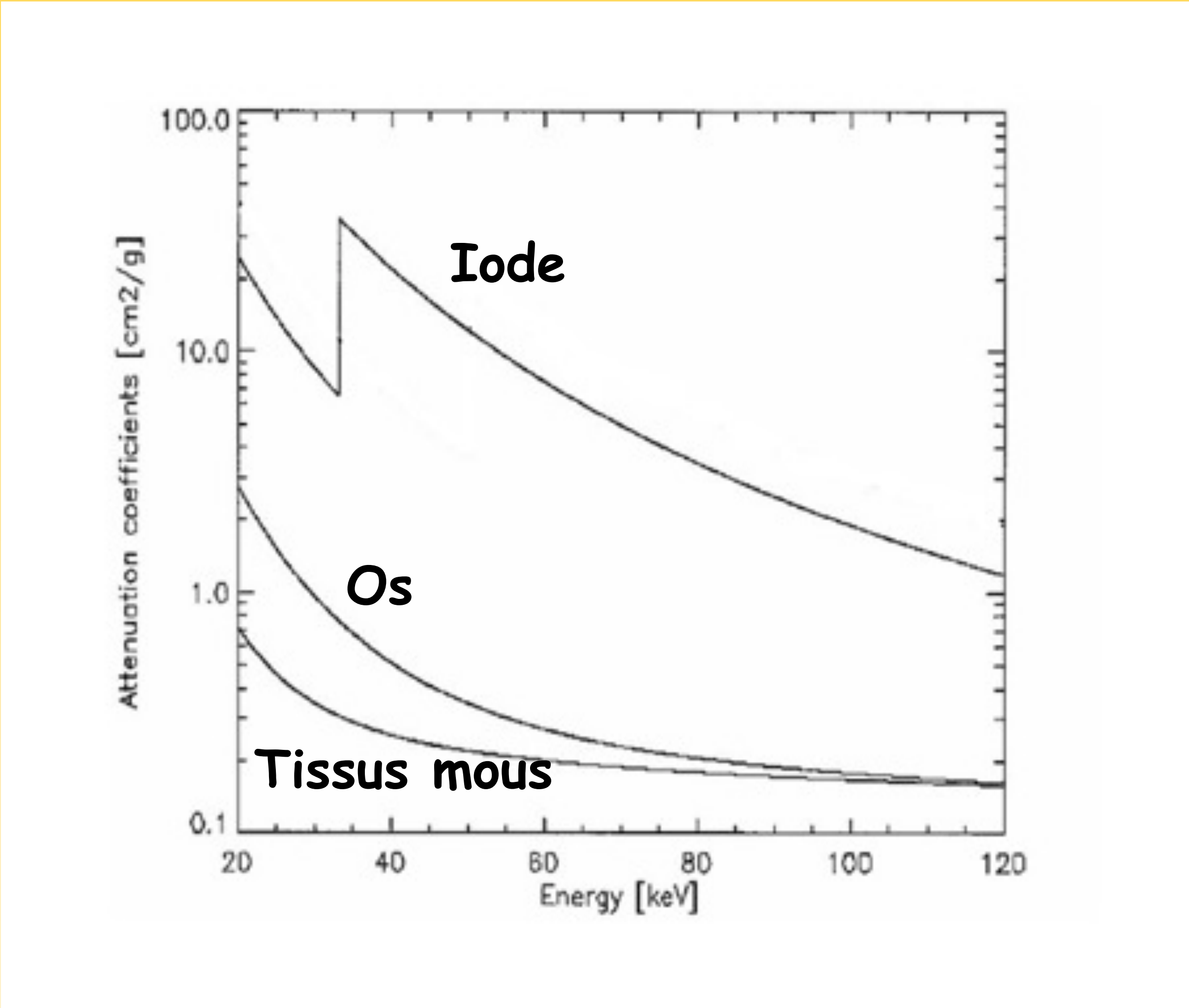

Go towards X-color imaging : concept

Contrast magnification

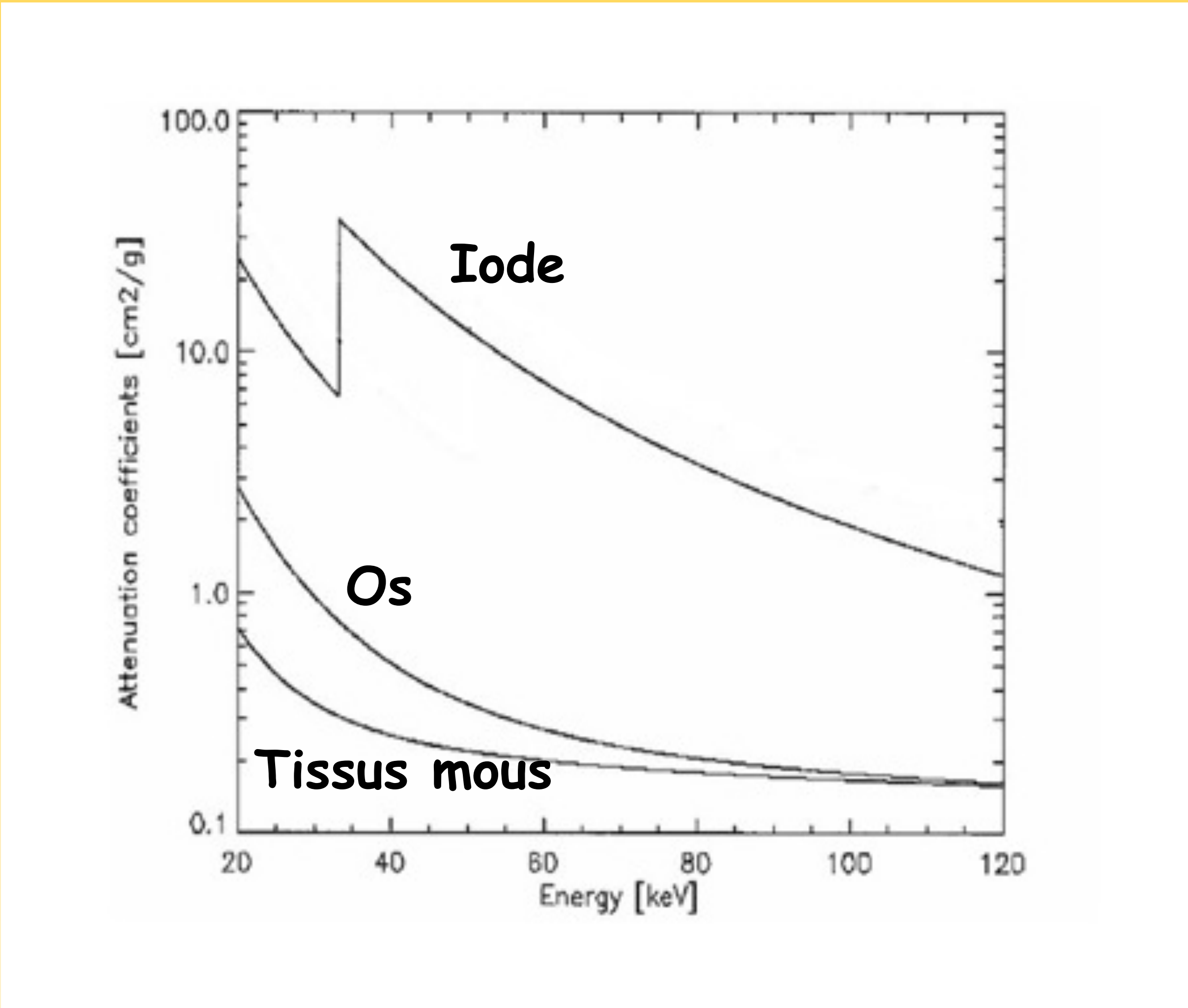

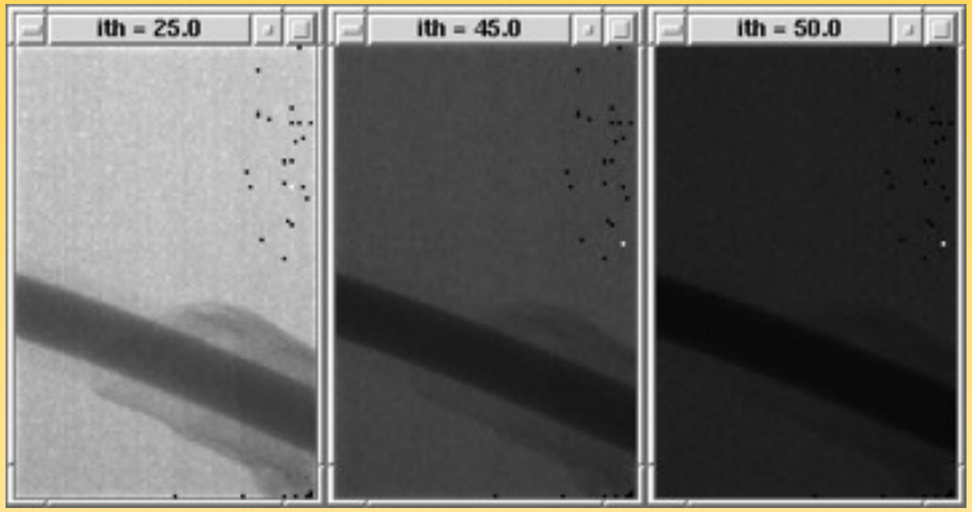

Go towards X-color imaging : concept

Contrast magnification

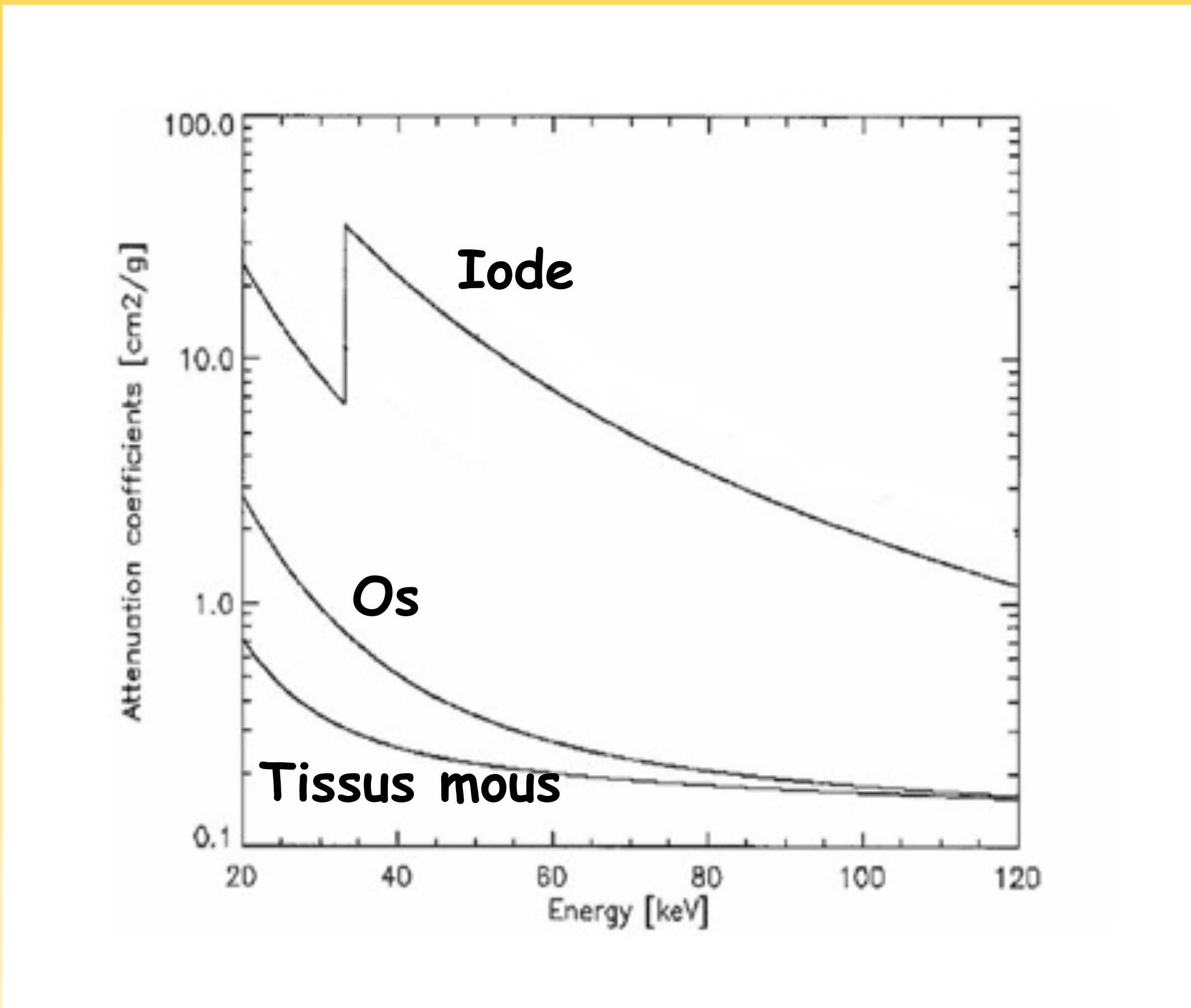

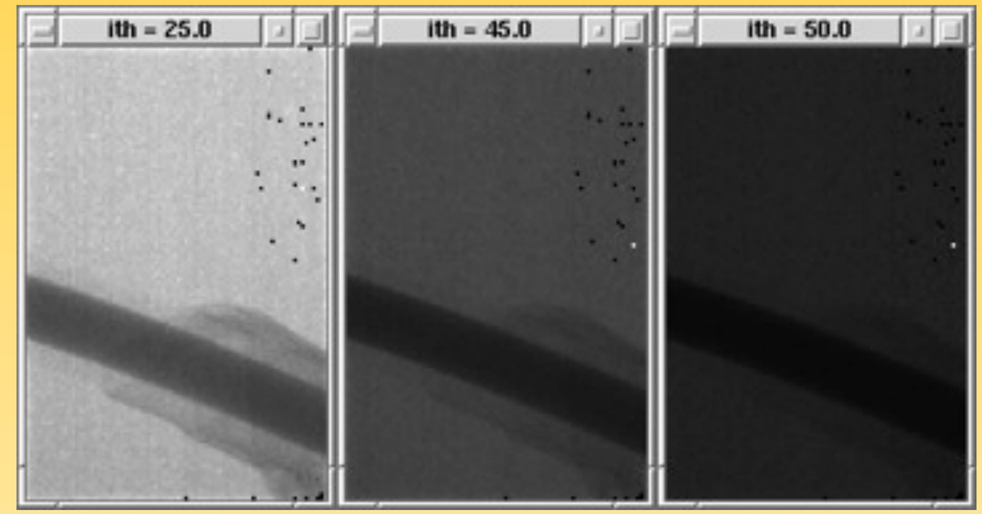

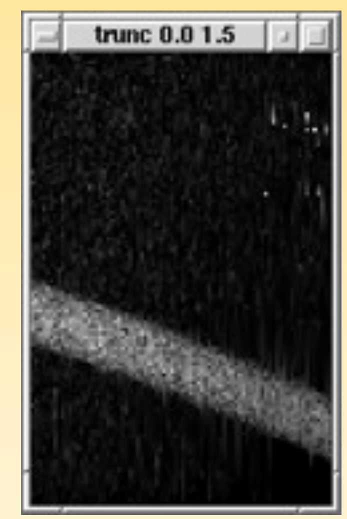

Go towards X-color imaging : concept

Capteur CdTe efficace jusqu'à 100 keV

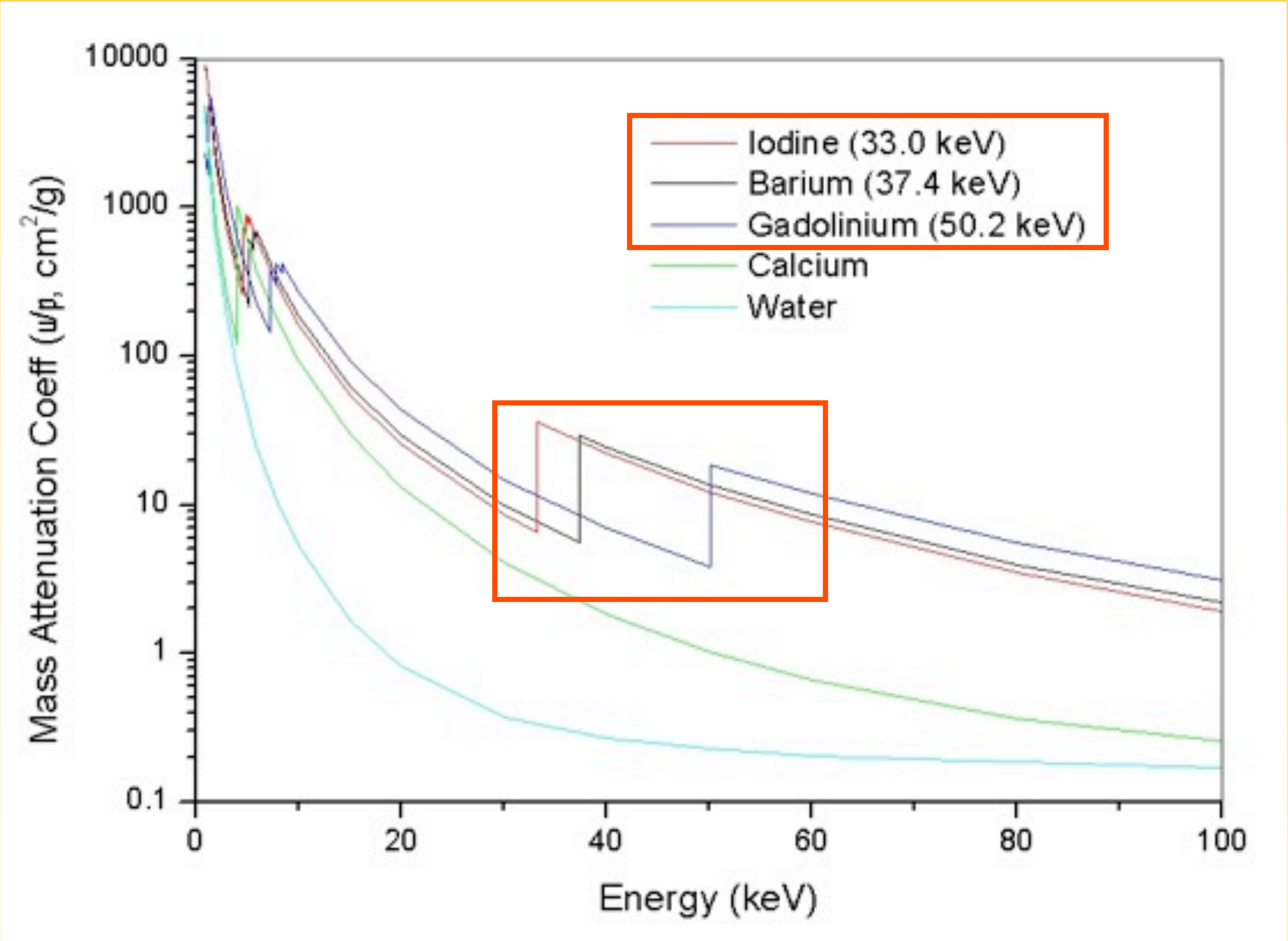

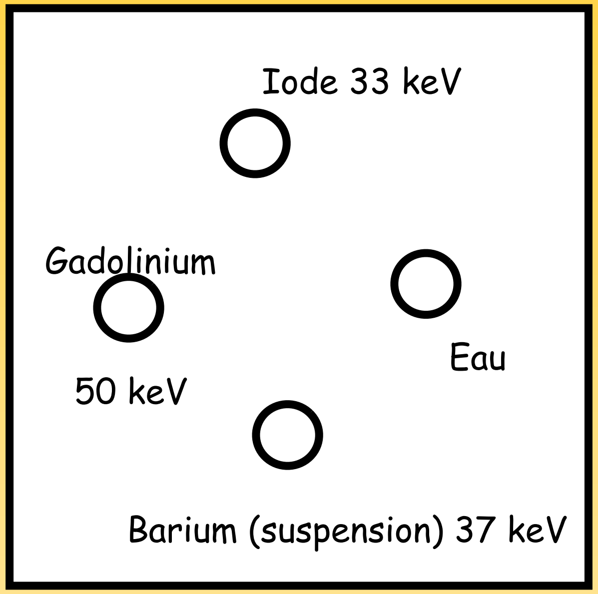

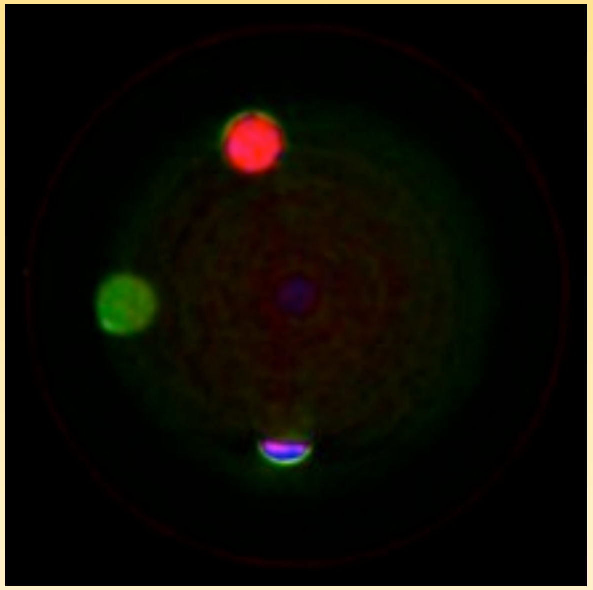

courtesy: A. Butler, MARS Biomedical Imaging Ltd.

3 pharmaceutiques, fantôme perspex

Université Albert-Ludwigs à Freiburg
et université de Canterbury

Go towards X-color imaging : concept

Iode : circulation pulmonaire

Barium : poumons

Calcium : os normaux

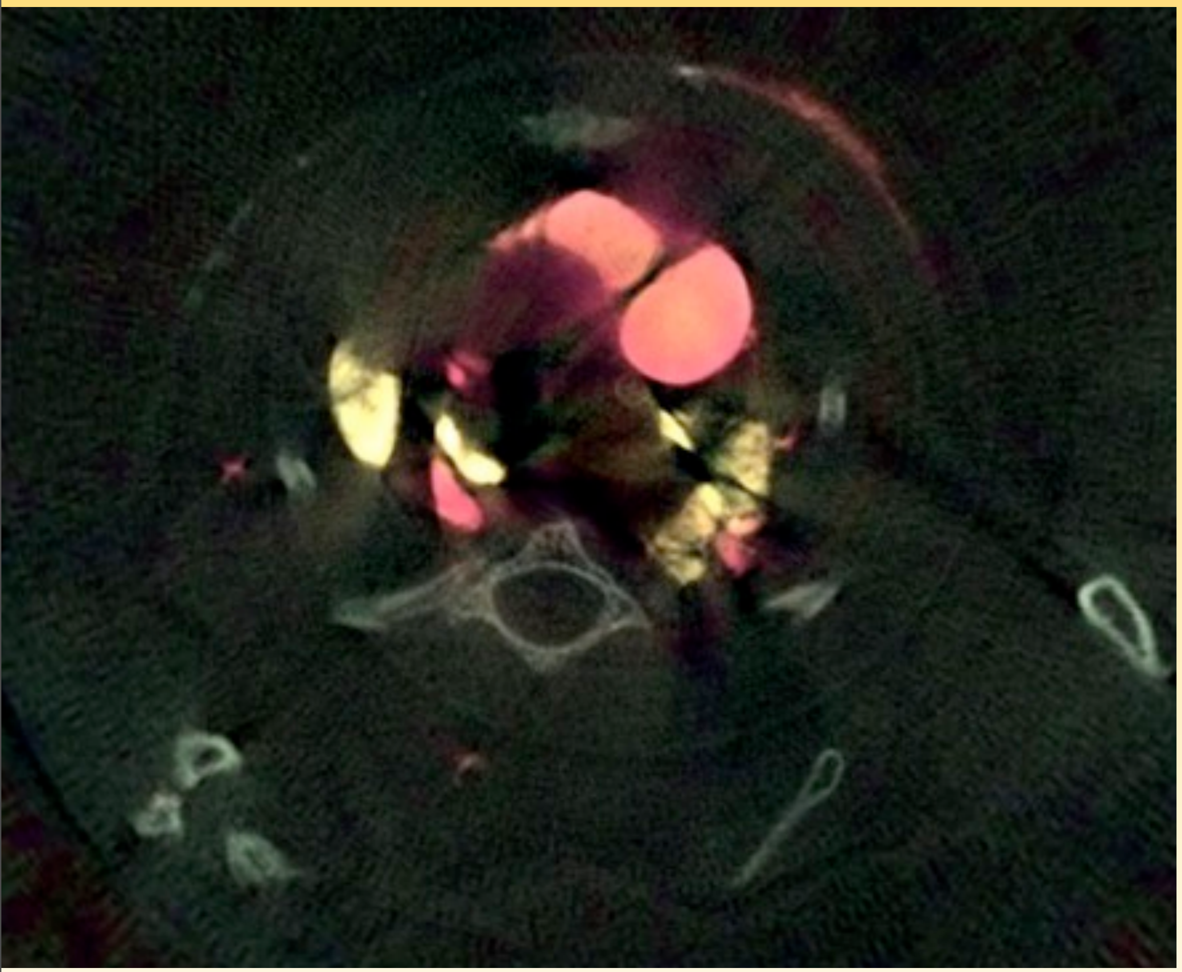

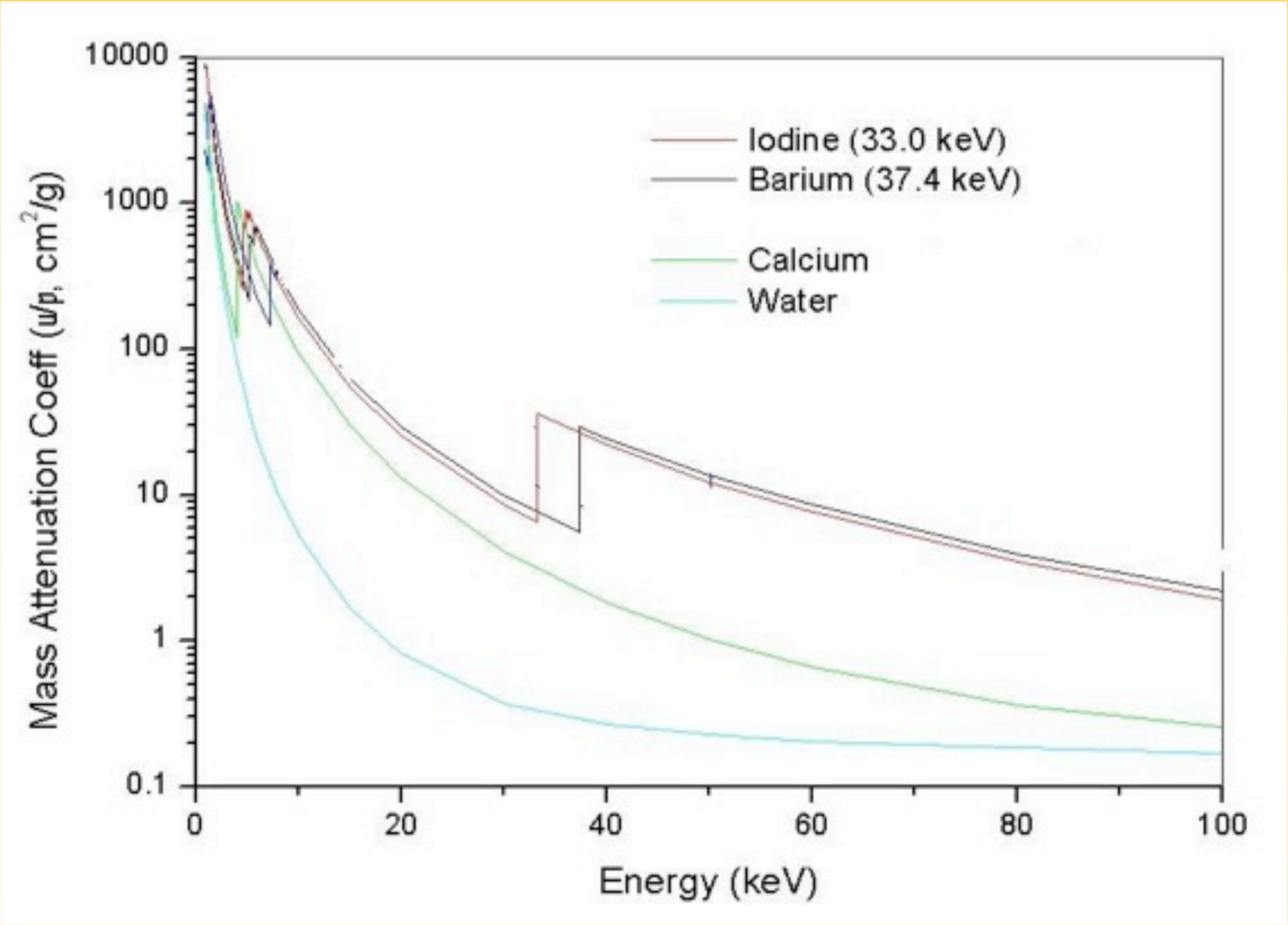

Système quantitatif developpé à l'université d'Erlangen-Nürnberg

courtesy: A. Butler, MARS Biomedical Imaging Ltd.

Towards Color Imaging : a Compressed Sensing framework ?

Measurements of spectra with different filters

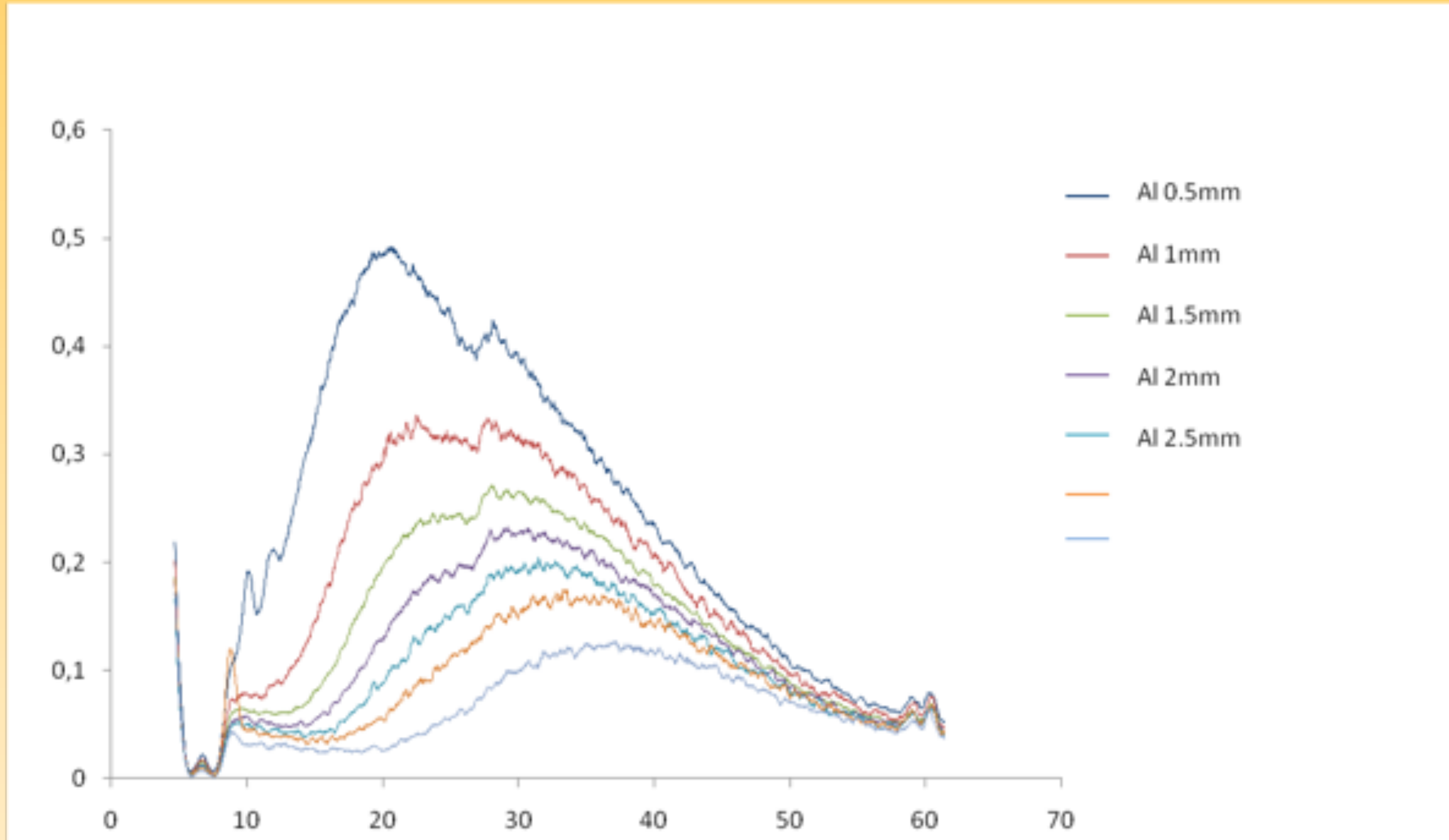

$$I_j(E) = I^0(E)e^{\left(-\int_{r_j}\mu(l,E)dl\right)} \qquad y_{j,T} = \int_T^{\infty} I_j(E)dE$$

No more (obvious) linearity ... sad news !

Conclusion

New XPAD3 hybrid pixels camera for X-ray photon counting developed at CPPM :

- CT-Scanner based on hybrid pixels.
- Simultaneous PET/CT scanner for bimodality images.

Simulations as well as real acquisitions have proven the reliability of hybrid pixels for micro-CT scanner and PET/CT !

Adapted algorithms :

- For low dose : Poisson noise to take into account
- For small number of projections : regularization needed ... sparsity basis ?
- For color imaging : adapt the acquisition framework ... CS theory for help ?

Implementation on GPUs strongly speeds-up the reconstruction (between 100 and 300 times faster compared to CPUs). To be implemented for iterative methods ?